Radboud Universiteit

From materials science to basic physics

Mikhail Katsnelson

1. Wave-particle duality in solids: itinerant vs localized behavior of electrons in correlated systems. How to understand ARPES data

2. Massless Dirac fermions in solids. Graphene as CERN on the desk: vacuum reconstruction, Klein paradox and all that

Instead of epigraph

You can get much further with a *kind word* and a *gun* than you can with a *kind word* alone
(Al Capone)

You can get much further with an insight from experiment and mathematics than you can with mathematics alone

Microworld: waves are corpuscles, corpuscles are waves

Einstein, 1905 – for light (photons)
L. de Broglie, 1924 – electrons and other microparticles

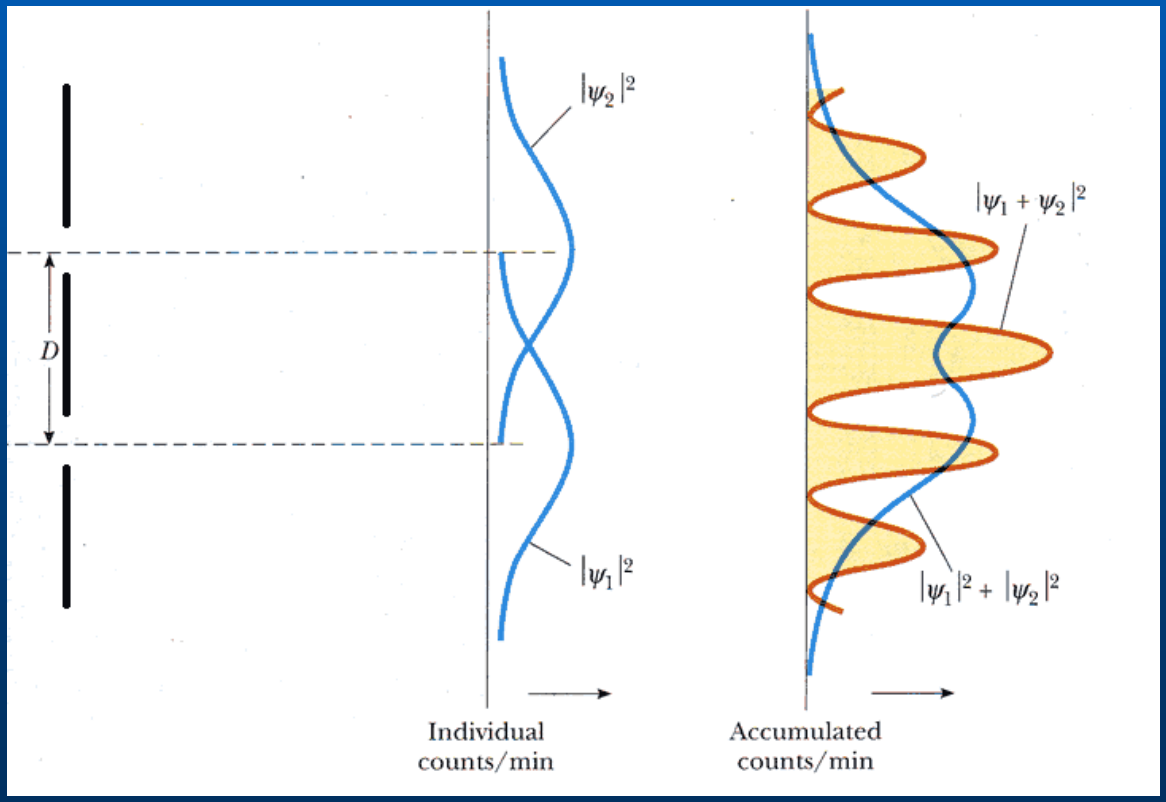

Electrons are particles (you cannot see half of electron) but moves along all possible directions (interference)

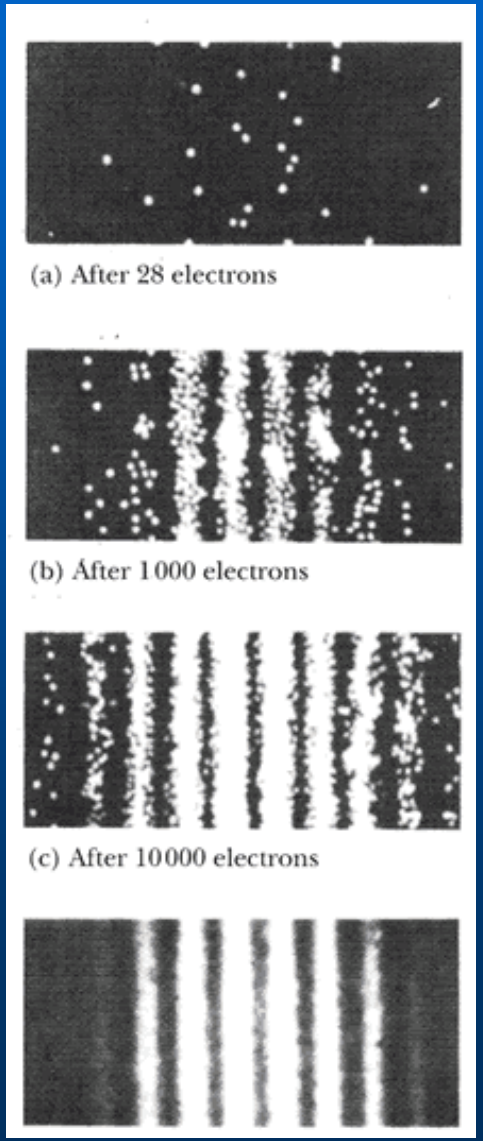

(a) After 28 electrons

(b) After 1000 electrons

(c) After 10000 electrons

Universal property of matter

Wave–particle duality of C_{60} molecules

Markus Arndt, Olaf Nairz, Julian Vos-Andreae, Claudia Keller, Gerbrand van der Zouw & Anton Zeilinger

NATURE | VOL 401 | 14 OCTOBER 1999

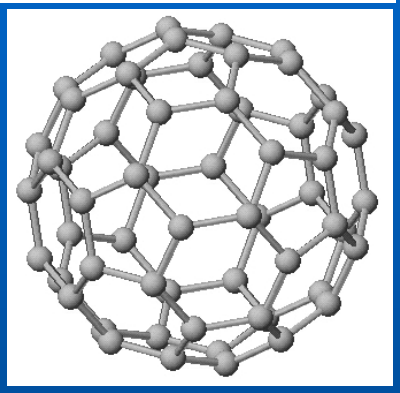

C_{60}

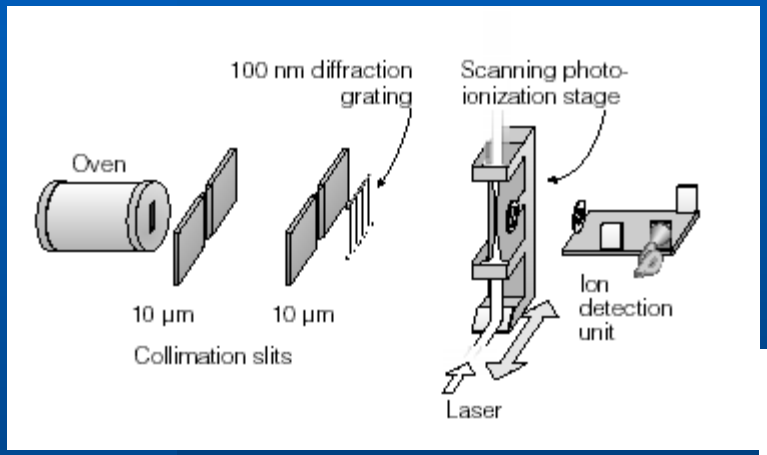

Matter waves for C_{60} molecules

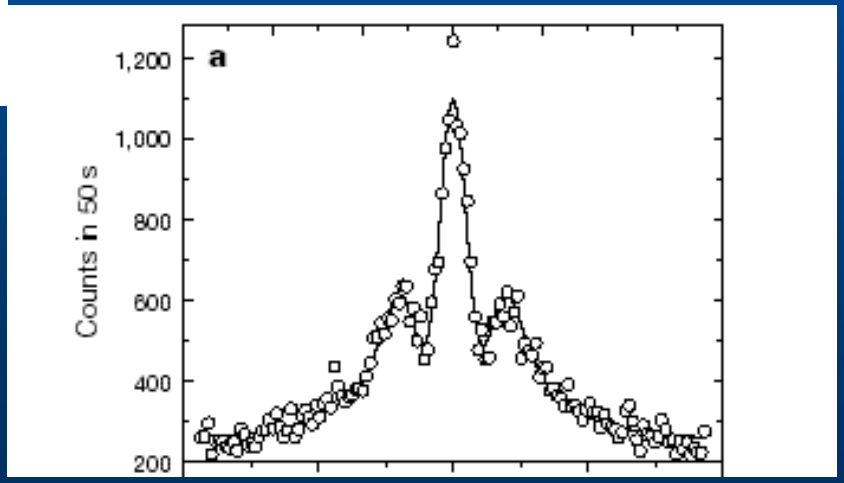

From atoms to solids

Atoms:

Electron-electron interaction plays crucial role

Optimal filling

Terms, multiplets

Hund's rules

Making solids from atoms: electrons at given site

How to combine?!

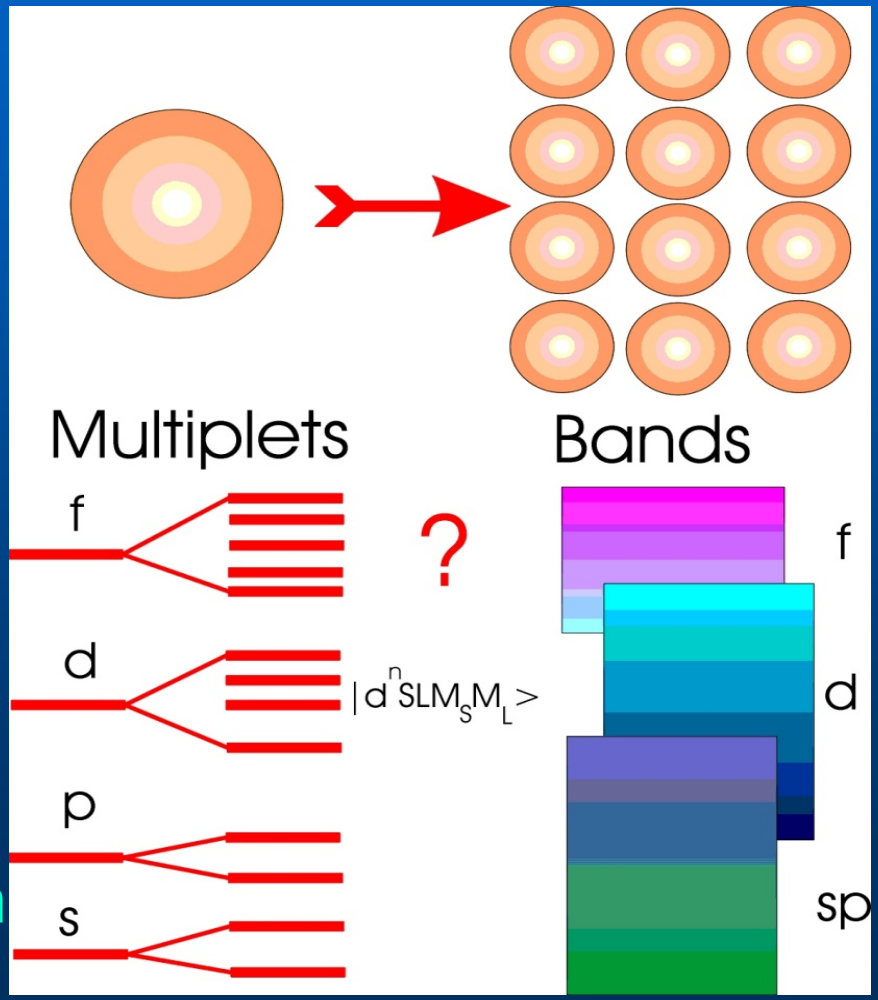

Crystals:

Bloch waves propagating through the crystal

Dispersion law

Fermi surface

Electron-electron Interaction just renormalizes parameters (Fermi liquid)...

The beginning: “Polar model”

On the Electron Theory of Metals.

By S. Schubin and S. Wonsowsky.

Sverdlovsk Physical Technical Institute.

(Communicated by R. H. Fowler, F.R.S.—Received December 29, 1933.)

Proc. R. Soc. Lond. A 1934 **145**, published 2 June 1934

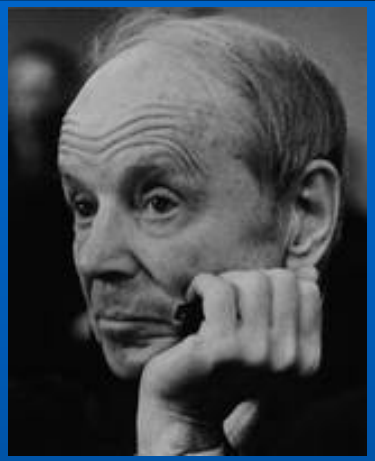

S. P. Shubin (1908-1938) S. V. Vonsovsky (1910-1998)

$$\int \frac{e^2}{|x-x'|}\,\phi_\alpha{}^2(x)\,\phi_\alpha{}^2(x')\,dx\,dx' = \mathrm{A}$$

$$\int \sum_{\gamma\neq\beta}\left[\mathrm{G}_\gamma(x)\,\phi_\alpha{}^2(x') + \frac{e^2}{|x-x'|}\,\phi_\gamma{}^2(x')\right]\phi_\alpha(x)\,\phi_\beta(x)\,dx\,dx' = \mathrm{L}_{\alpha\beta}$$

$$\int \frac{e^2}{|x-x'|}\,\phi_\alpha{}^2(x)\,\phi_\beta{}^2(x')\,dx\,dx' = \mathrm{B}_{\alpha\beta}$$

$$\int \frac{e^2}{|x-x'|}\,\phi_\alpha(x)\,\phi_\beta(x)\,\phi_\alpha(x')\,\phi_\beta(x')\,dx\,dx' = \mathrm{J}_{\alpha\beta}$$

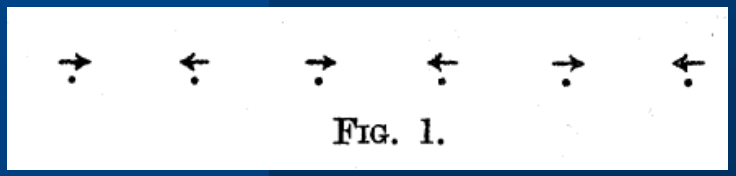

Fig. 1.

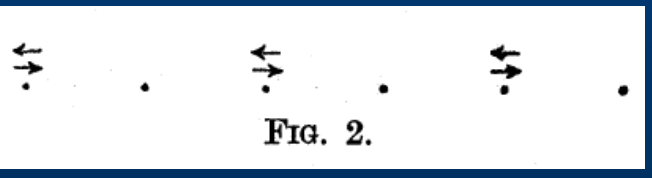

Fig. 2.

The beginning: "Polar model" II

Schrödinger equation in "atomic representation" (double *f*, hole *g*, spin right *k*, spin left *h*)

$$\{\varepsilon - s(A+D) - [\sum_{f<f'}(B_{ff'} - J_{ff'}) + \sum_{g<g'}(B_{gg'} - J_{gg'}) - \sum_{f,g}(B_{fg} + J_{fg})]\}C(fgh)$$
$$+ \sum_{h,k} J_{hk}[C(T_{hk}|fgh) - C(fgh)] + \sum_{f,g} J_{fg}[C(T_{fg}|fgh) - C(fgh)]$$
$$+ \sum_{f,p} L_{fp} C(T_{fp}|fgh) - \sum_{g,p} L_{gp} C(T_{gp}|fgh) = 0, \qquad (9)$$

Metal-insulator transition and Mott insulators

(II). The minimum energy corresponds to a certain $s = s_0$, where $0 < s_0 < n$. This case we have, for instance, when

$$A + 6(J - B) > 0, \quad A + 6J - 12L < 0.$$

Then, so long as s remains small, the lowest energy level *diminishes* as s increases; for a certain $s = s_0$ it attains a minimum and then again begins to increase. For such metals—at not very high temperatures—the number of "free" electrons approximates to twice this s_0 (electrons + holes !) and is therefore *smaller* than the number of atoms. In order to calculate s_0 in terms of our integrals, the energy must be evaluated up to the second approximation in powers of s/n; we shall not, however, make these rather cumbersome calculations here.

Metal

Insulator

(III). The minimum energy corresponds to $s = 0$. This is the case when

$$A + 6(J - B) > 0, \quad A + 6J - 12L > 0.$$

When do we have a problem?

sp metals (empty or completely filled df shells): purely itinerant behavior

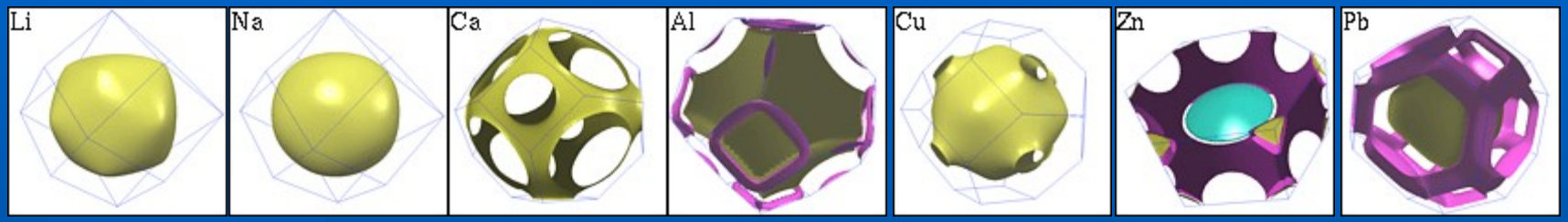

http://www.phys.ufl.edu/fermisurface/periodic_table.html

4f (rare earth) metals: *f* electrons are atomic like, *spd* electrons are itinerant

PHYSICAL REVIEW B **74**, 045114 (2006)

Multiplet effects in the electronic structure of light rare-earth metals

S. Lebègue,[1,2] A. Svane,[3] M. I. Katsnelson,[4] A. I. Lichtenstein,[5] and O. Eriksson[1]

Photoemission (red) and inverse photoemissin (green)

PES

$f^5 \rightarrow f^4$

$^5I_4$, ^5F, ^5G, and ^5D final states

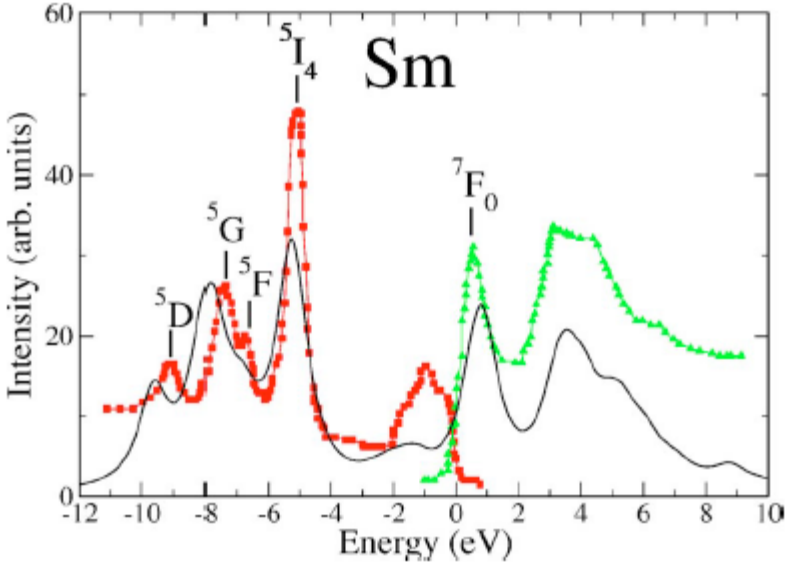

Itinerant-electron magnets: coexistence

Fe

Co

Ni

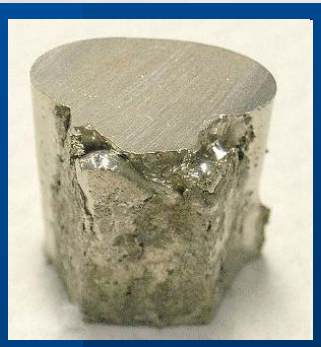

Iron, majority spin FS

Local magnetic moments do exist above T_C (Curie-Weiss law, spectroscopy, neutrons…)

d electrons are itinerant (FS, chemical bonding, transport…)

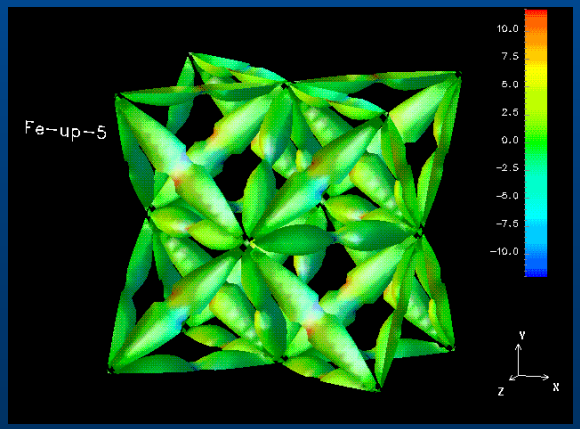

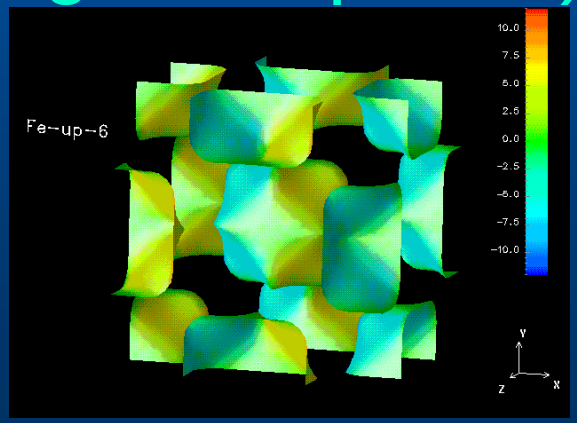

4f electrons are normally pure localized but not 3d

From atomic state to itinerant

PRL **104,** 117601 (2010) PHYSICAL REVIEW LETTERS week ending 19 MARCH 2010

Correlated Electrons Step by Step: Itinerant-to-Localized Transition of Fe Impurities in Free-Electron Metal Hosts

C. Carbone,[1] M. Veronese,[1] P. Moras,[1] S. Gardonio,[1] C. Grazioli,[1] P. H. Zhou,[2] O. Rader,[3] A. Varykhalov,[3] C. Krull,[4] T. Balashov,[4] A. Mugarza,[4] P. Gambardella,[4,5] S. Lebèque,[6] O. Eriksson,[7] M. I. Katsnelson,[8] and A. I. Lichtenstein[9]

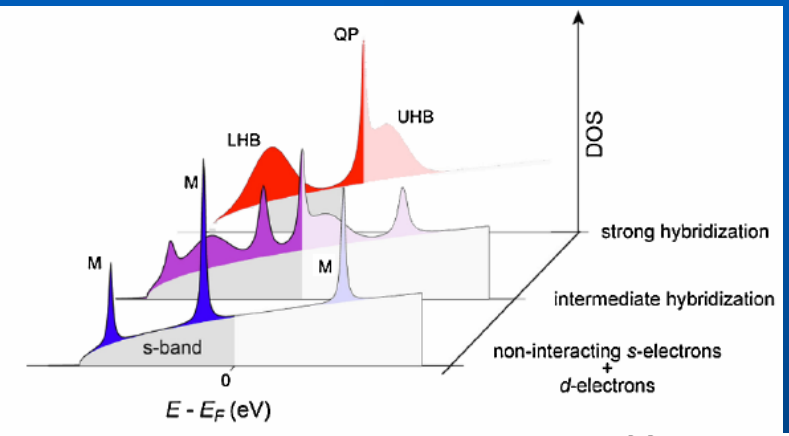

Experiment: disappearance of multiplets

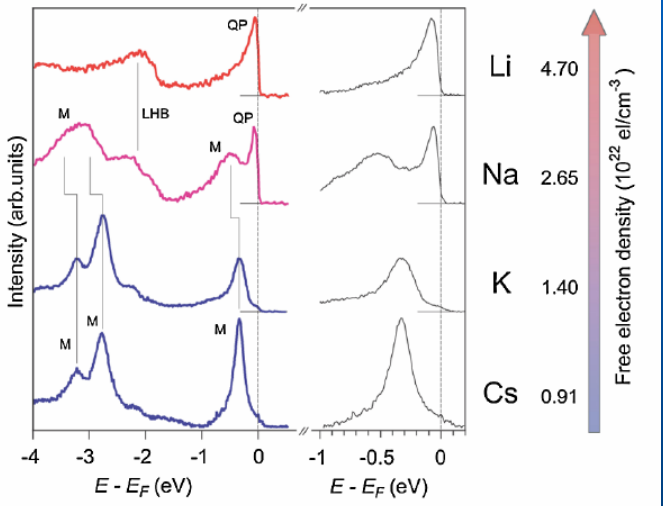

Calculations: increase of hybridization

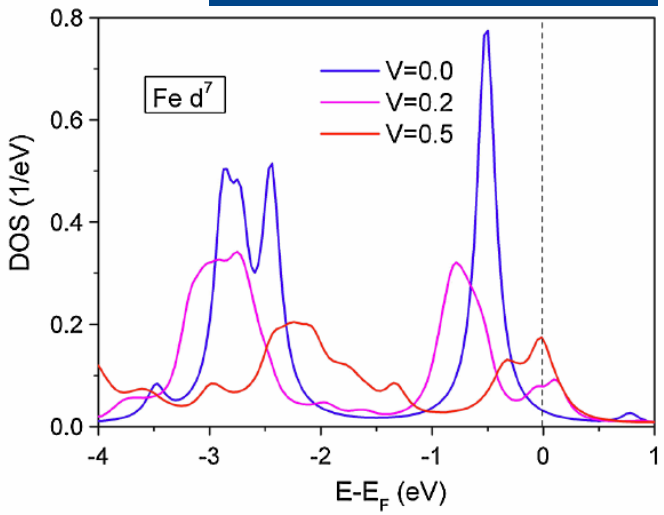

Blue line: exact diagonalization for free atom

Dynamical Mean Field Theory

A.Georges, G.Kotliar, W.Krauth and M.Rozenberg, Rev. Mod. Phys. '96

A natural generalization of the familiar MFT
to the problem of electrons in a lattice

Key idea: take one site out of a lattice and embed it in a self-consistent bath = mapping to an effective impurity problem

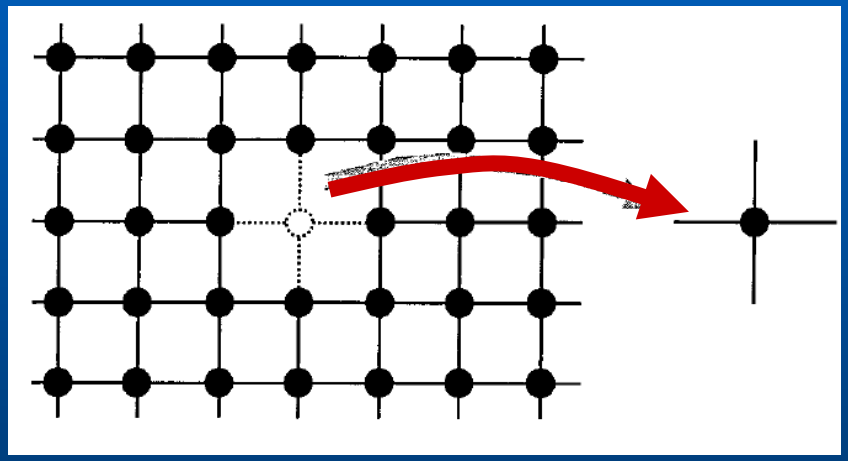

Effective impurity: atomic-like features, many-body problem

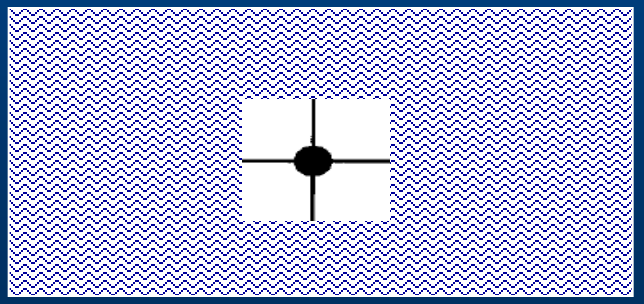

Putting into crystal: itinerant features, single-body problem

Combination with realistic calculations

A.Lichtenstein and MIK, PRB 57, 6884 (1998); JPCM 11, 1037 (1999)
V.Anisimov et al, JPCM 9, 7339 (1997)

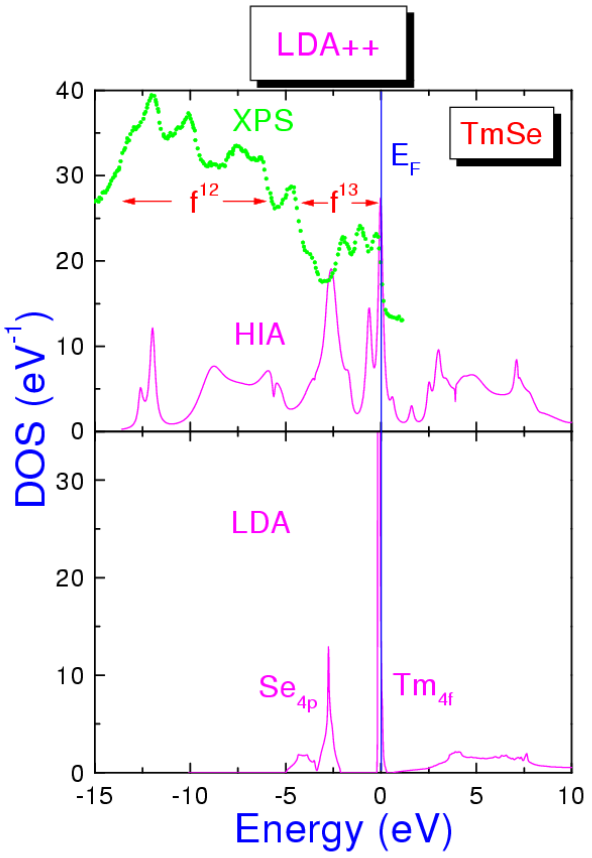

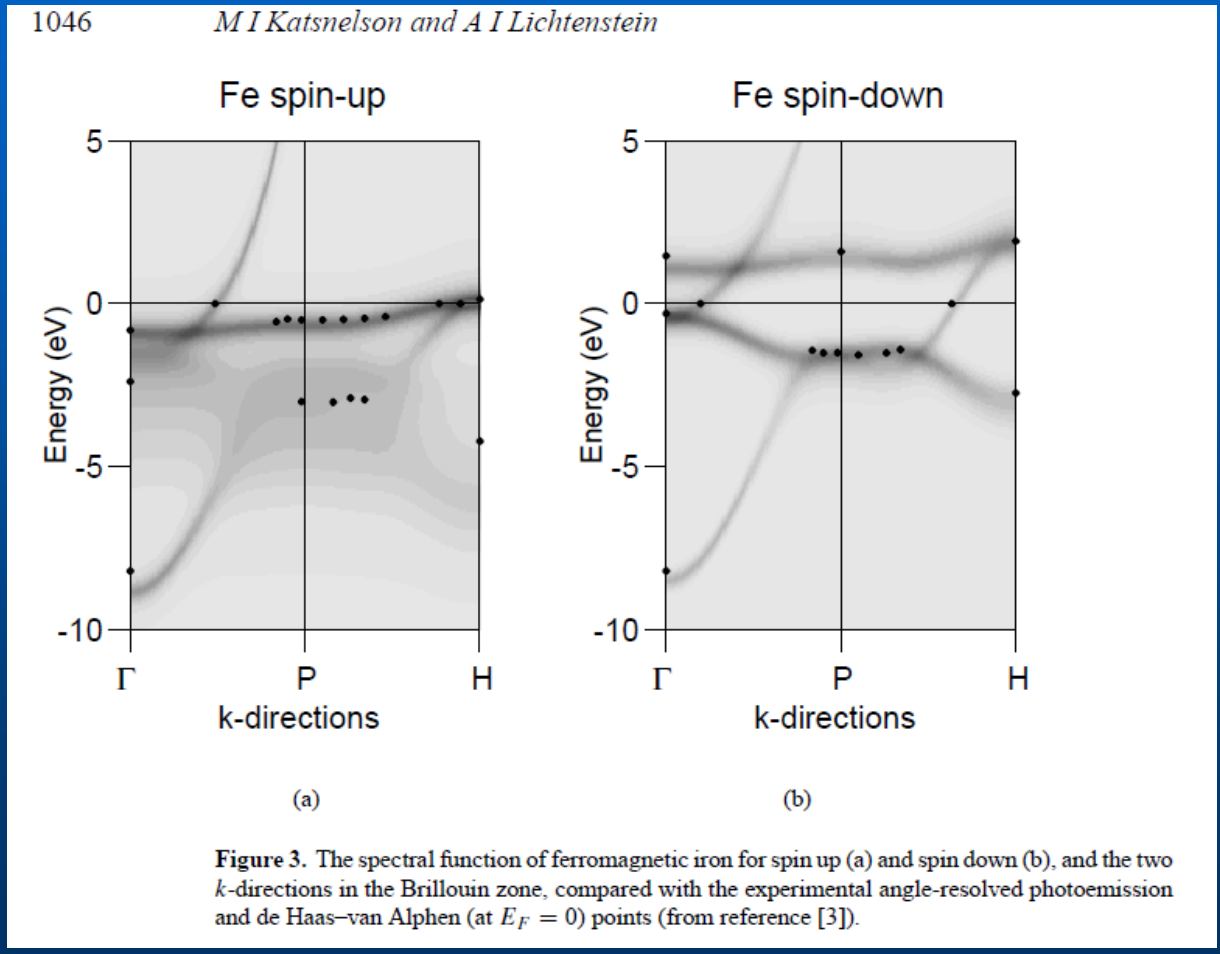

Figure 3. The spectral function of ferromagnetic iron for spin up (a) and spin down (b), and the two k-directions in the Brillouin zone, compared with the experimental angle-resolved photoemission and de Haas–van Alphen (at $E_F = 0$) points (from reference [3]).

PRB 57, 6884 (1998)

JPCM 11, 1037 (1999)

Ferromagnetism of transition metals: LDA+DMFT

Ferromagnetic Ni DMFT vs. LSDA:

- 30% band narrowing
- 50% spin-splitting reduction
- -6 eV sattellite

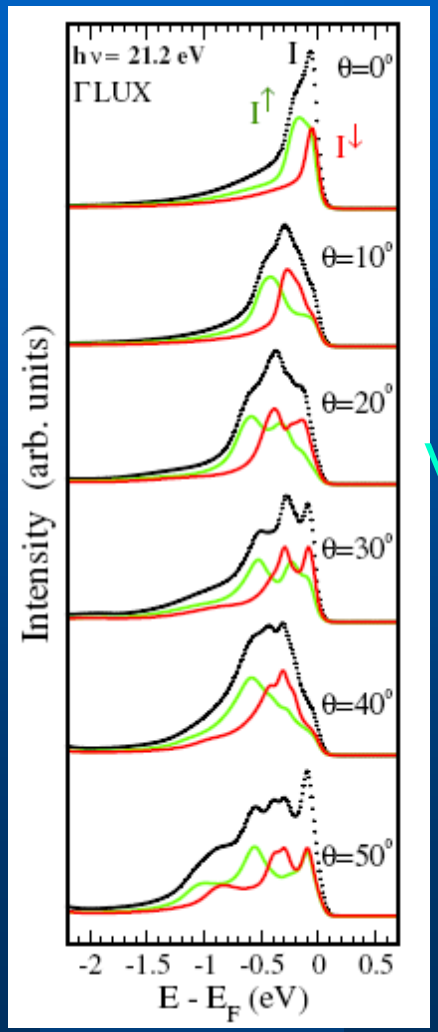

LDA+DMFT with ME
J. Braun *et al*
PRL (2006)

Very good for Ni

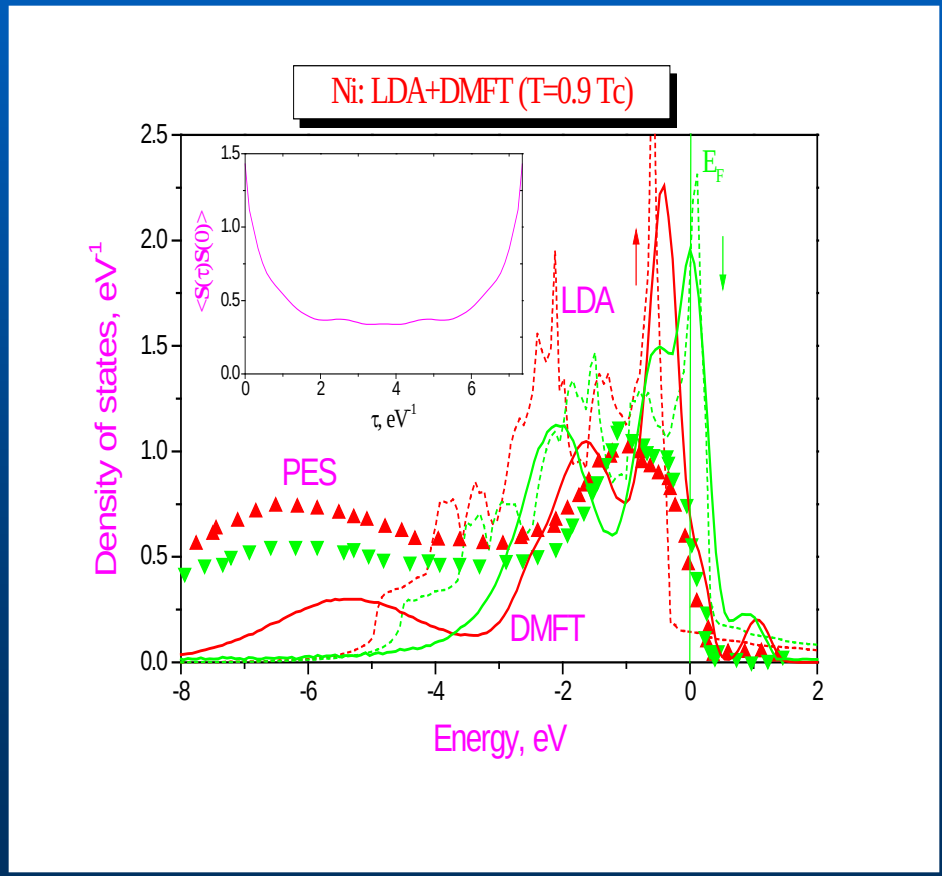

Lichtenstein, MIK, Kotliar, PRL (2001)

ARPES for iron

PRL **103,** 267203 (2009) PHYSICAL REVIEW LETTERS week ending 31 DECEMBER 2009

Strength of Correlation Effects in the Electronic Structure of Iron

J. Sánchez-Barriga,[1] J. Fink,[1,2] V. Boni,[3] I. Di Marco,[4,5] J. Braun,[6] J. Minár,[6] A. Varykhalov,[1] O. Rader,[1] V. Bellini,[3] F. Manghi,[3] H. Ebert,[6] M. I. Katsnelson,[5] A. I. Lichtenstein,[7] O. Eriksson,[4] W. Eberhardt,[1] and H. A. Dürr[1]

Agreement is not bad (much better than LDA/GGA) but essentially worse than in nickel. Correlations in iron are not quite local

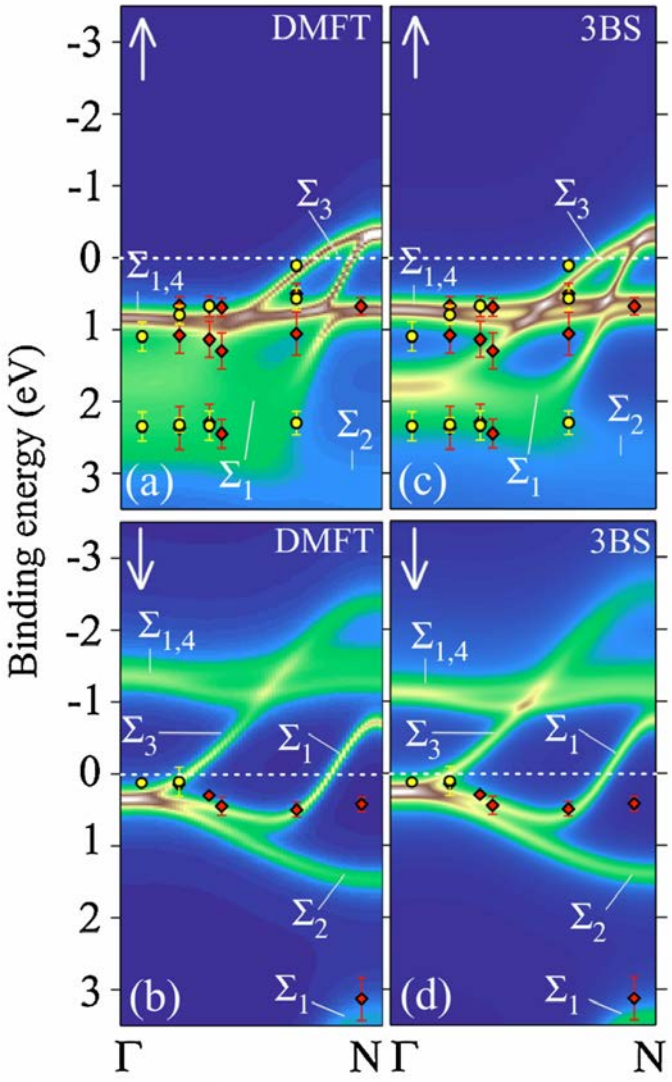

ARPES for 3d metals

PHYSICAL REVIEW B **85**, 205109 (2012)

Effects of spin-dependent quasiparticle renormalization in Fe, Co, and Ni photoemission spectra: An experimental and theoretical study

J. Sánchez-Barriga,[1] J. Braun,[2] J. Minár,[2] I. Di Marco,[3] A. Varykhalov,[1] O. Rader,[1] V. Boni,[4] V. Bellini,[5] F. Manghi,[4] H. Ebert,[2] M. I. Katsnelson,[6] A. I. Lichtenstein,[7] O. Eriksson,[3] W. Eberhardt,[1] H. A. Dürr,[1,8] and J. Fink[1,9]

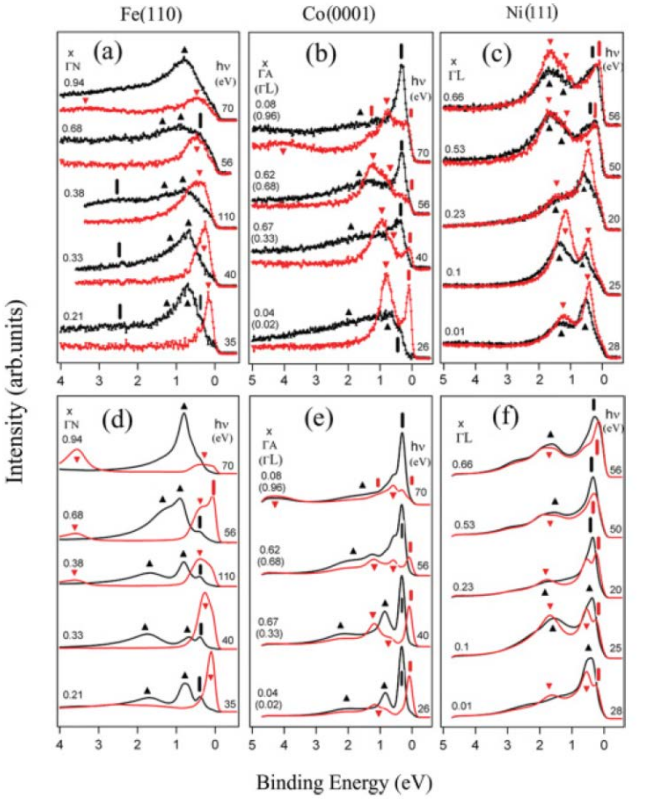

Variation of U does not help too much for Fe

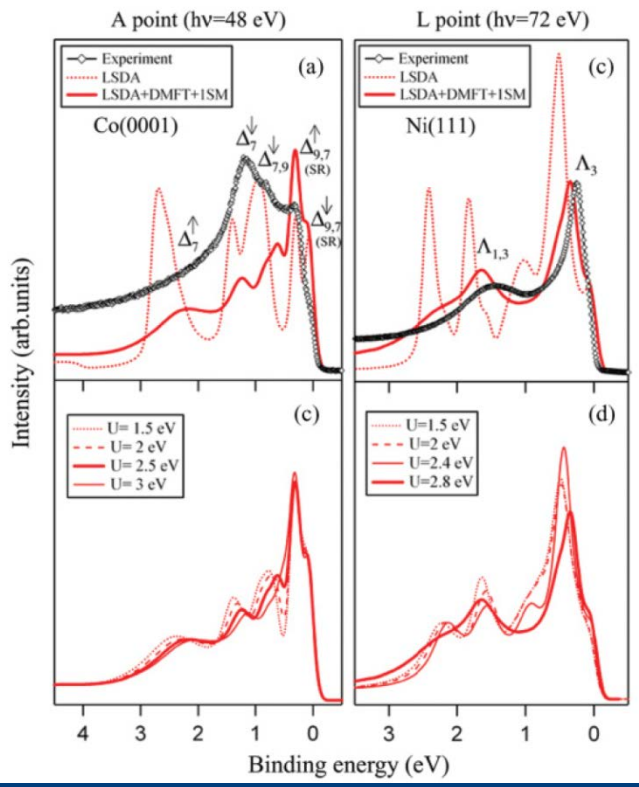

Black – spin up, red – spin down
Upper panel – exper,lower - DMFT

TABLE I. Values of the experimental and theoretical mass enhancement factors m^*/m_0 for majority spin states at high symmetry points of the BBZ of Fe, Co, and Ni, respectively. The theoretical values are derived for $U(\mathrm{Fe}) = 1.5$ eV, $U(\mathrm{Co}) = 2.5$ eV, $U(\mathrm{Ni}) = 2.8$ eV.

Fe			Co			Ni		
	Expt.	Theory		Expt.	Theory		Expt.	Theory
Γ	1.7	1.2	Γ	1.26	1.31	Γ	2.0	1.8
N	1.1	1.2	A	1.29	1.31	Λ	1.9	1.8

How to go beyond DMFT: Dual fermion approach

A complicated change of variables in path integral such that DMFT becomes your new bare (noninteracting) Green's function

Rubtsov, MIK, Lichtenstein 2008

The price: interaction action is now more ugly (but hopefully small)

Sometimes frogs are better

Very good zeroth-order approximation (exact in both weak and strong coupling limits); perturbation only in nonlocal correlations

Technically speaking: ladder diagram summation is good

Applications to single-band Hubbard model

Example: Fermi condensation at the Van Hove filling

PRL 112, 070403 (2014) PHYSICAL REVIEW LETTERS week ending 21 FEBRUARY 2014

Fermi Condensation Near van Hove Singularities Within the Hubbard Model on the Triangular Lattice

Dmitry Yudin,[1] Daniel Hirschmeier,[2] Hartmut Hafermann,[3] Olle Eriksson,[1]
Alexander I. Lichtenstein,[2] and Mikhail I. Katsnelson[4,5]

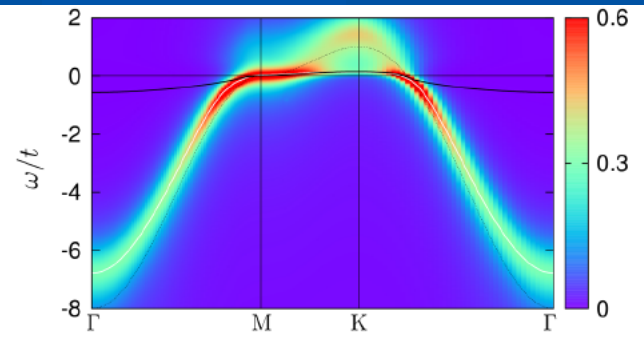

FIG. 3 (color online). Spectral function in dual fermion approach at $U/t = 8$ and $T/t = 0.05$. Local maxima corresponding to the lower band are indicated by a white line. In the vicinity of the Fermi level, this lower band perfectly matches the prediction $\varepsilon_{\mathbf{k}} - \mu = T \ln[(1 - n_{\mathbf{k}})/n_{\mathbf{k}}]$ following from the Fermi condensate hypothesis (thick black line). The bare dispersion is shown for comparison (blue, dashed).

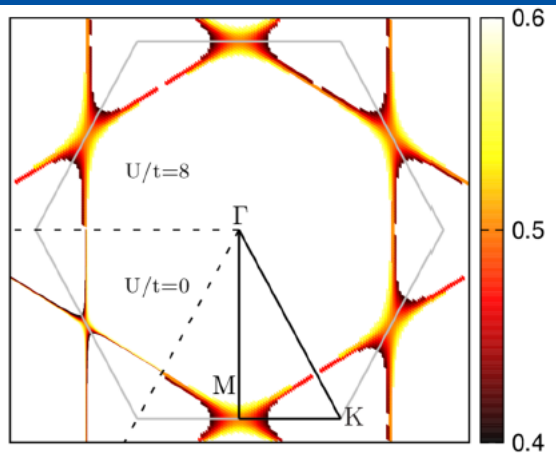

FIG. 4 (color online). Broadened Fermi surface within ±0.1 electrons for $U/t = 8$ and $T/t = 0.1$. The lower left sextant shows the noninteracting result.

Hope: to do multiband case and apply to Fe complicated but purely technical problem

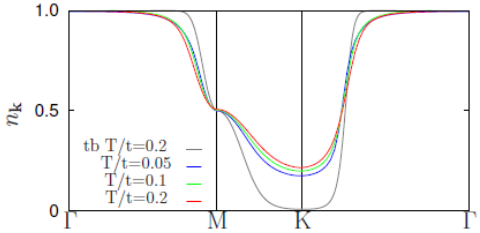

Experiments with ultracold gases

DF for Real Materials: Layered Cobaltate

PHYSICAL REVIEW B **91**, 155114 (2015)

From Hubbard bands to spin-polaron excitations in the doped Mott material Na_xCoO_2

Aljoscha Wilhelm,[1] Frank Lechermann,[1] Hartmut Hafermann,[2] Mikhail I. Katsnelson,[3] and Alexander I. Lichtenstein[1]

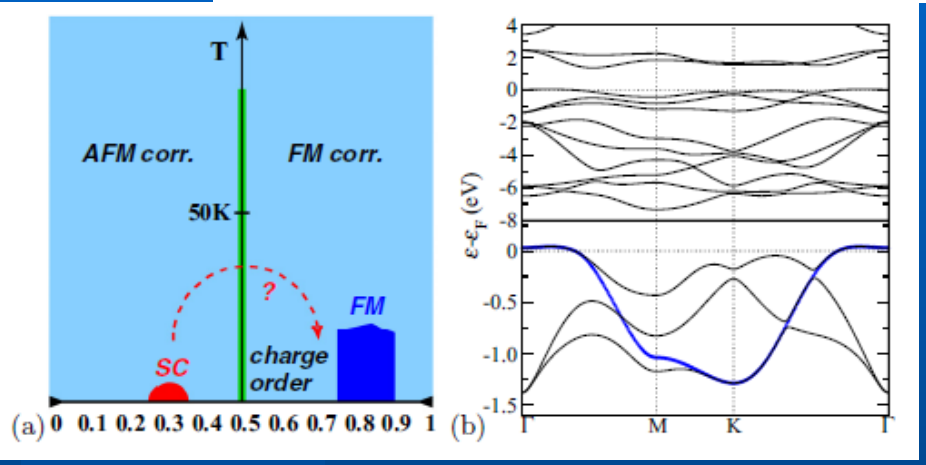

The model: mapping on a_{1g} band only (blue). Giant VHS – should be the main effect. Dual fermions in ladder approximation

Physics: bound state (spin polaron) in FM *t-J* model (MIK 1982)

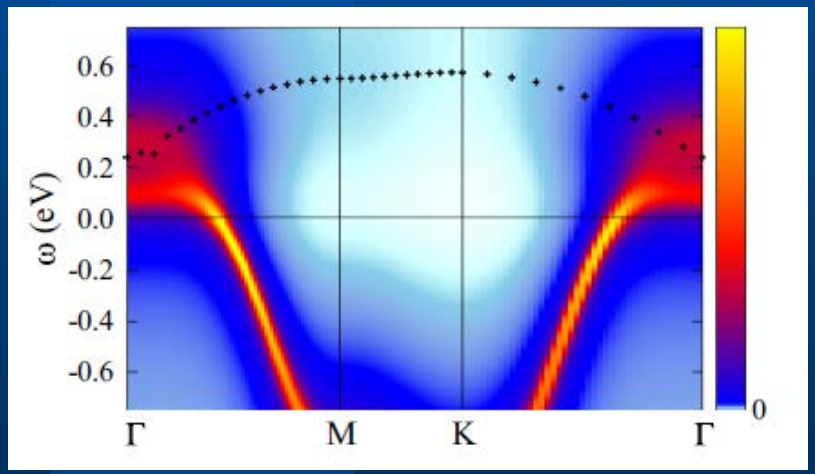

Band splitting beyond DMFT

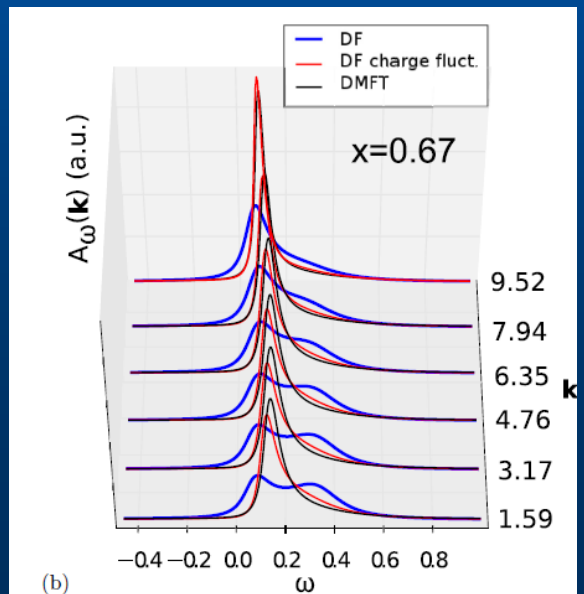

5f electrons: localized vs itinerant

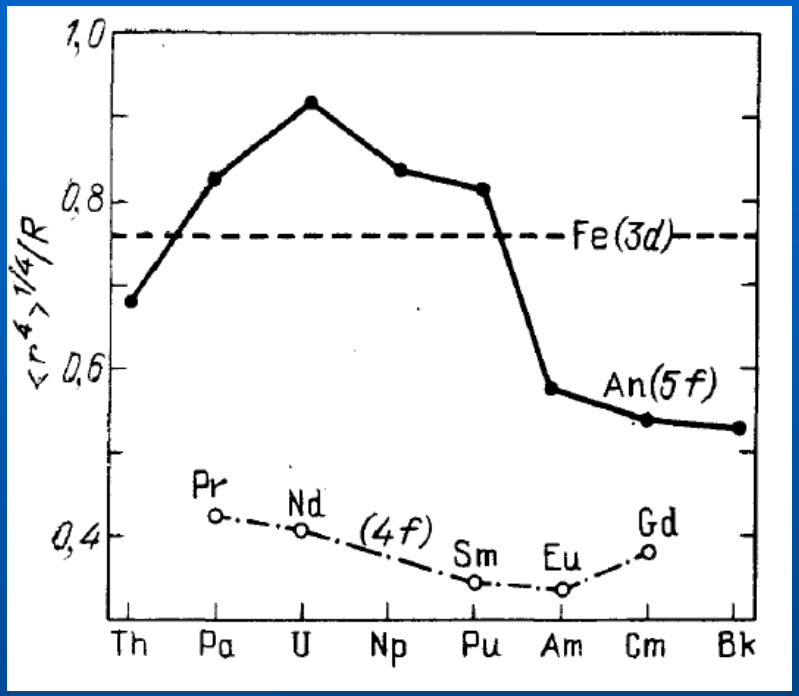

Ratio of radius of f states to the half of interatomic distance in elemental solids

Magnetism of uranium compounds: Hill criterion

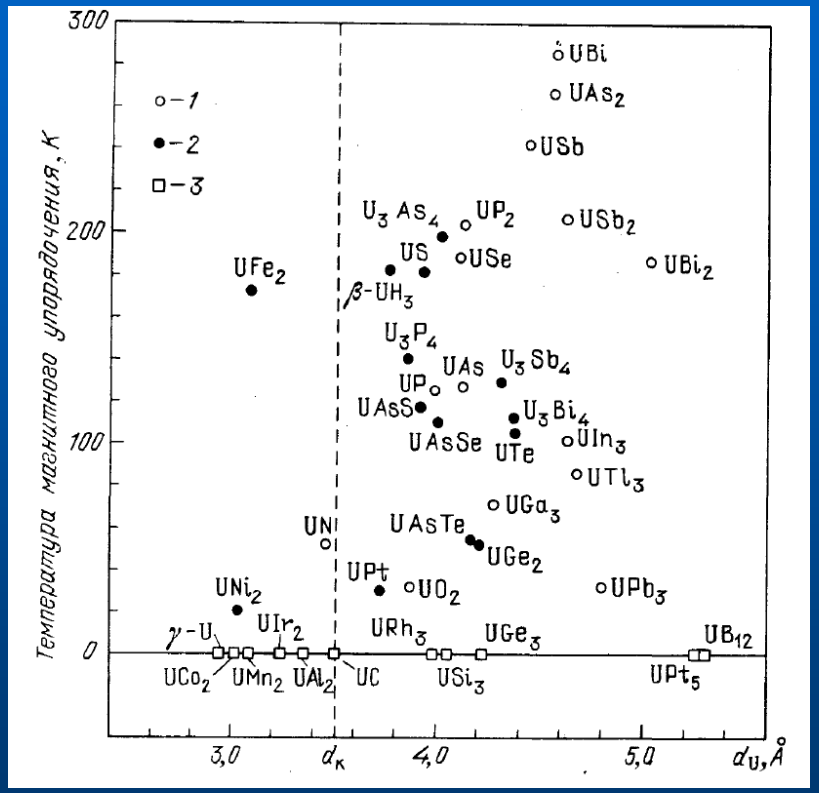

1- PM, 2- FM, 3 – AFM
(similar for Pu and Np compounds)

Localized-delocalized transition at d ≈ 3.5Å

Elemental Pu

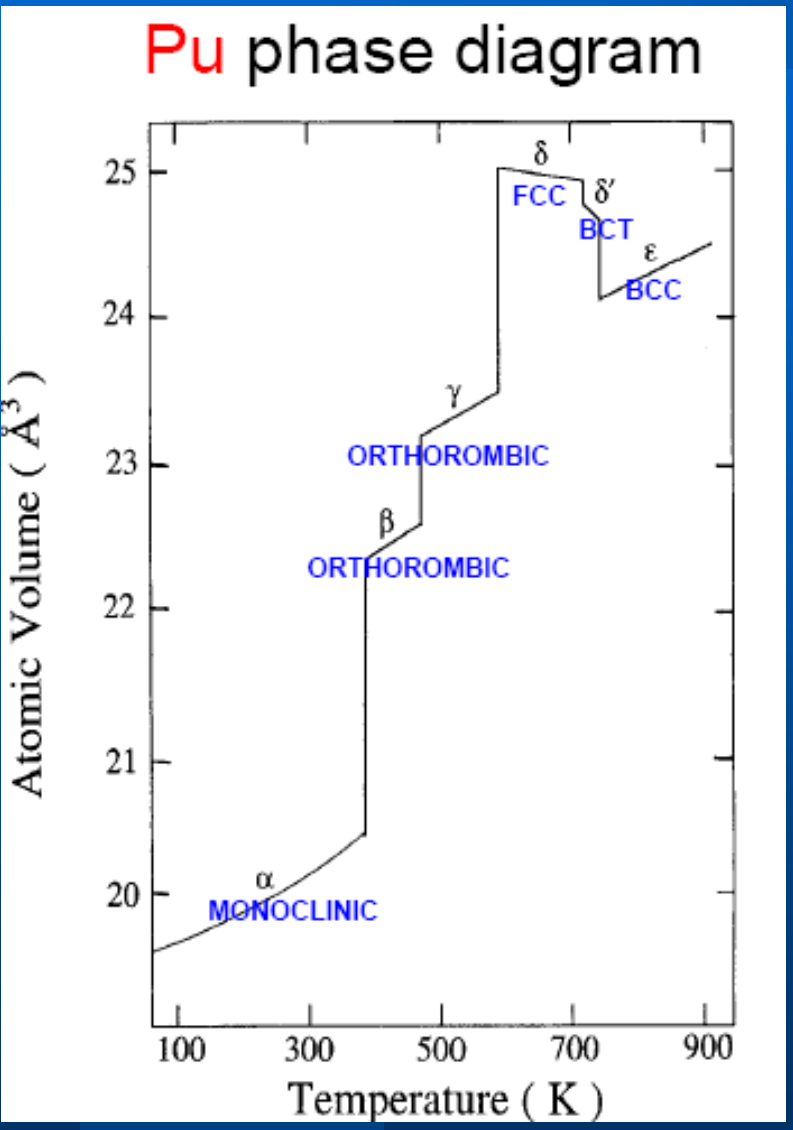

1. Six stable crystal phases at p=0
2. Negative thermal expansion in delta (fcc)-phase
3. Stabilization of delta' phase on the way of Bain (fcc-bcc) deformation
4. Huge volume jumps at phase Transitions (very unusual for metals, the only othe examples are alpha-gamma transition in Ce and "electronic" (s-d) transition in Cs at p = 43 kbar

Probably, the most interesting element in Periodic Table. Well... After carbon (and iron?!).

Elemental Pu II

α-δ transition in plutonium as a Mott transition in an *f* subsystem

M. I. Katsnel'son and I. V. Solov'ev
Institute of Metal Physics, Ural Branch of the Russian Academy of Sciences, 620219, Ekaterinburg, Russia

A. V. Trefilov
I. V. Kurchatov Institute of Atomic Energy, 123482, Moscow, Russia

(Submitted 31 July 1992)
Pis'ma Zh. Eksp. Teor. Fiz. **56**, No. 5, 276–279 (10 September 1992)

Based on idea of atomic collapse and LDA:

Transition is not between Pu and Am but between different phases of Pu

Evidences of localized-delocalized transition: width of canonical f-bands and sensitivity of magnetism to the type of magnetic order

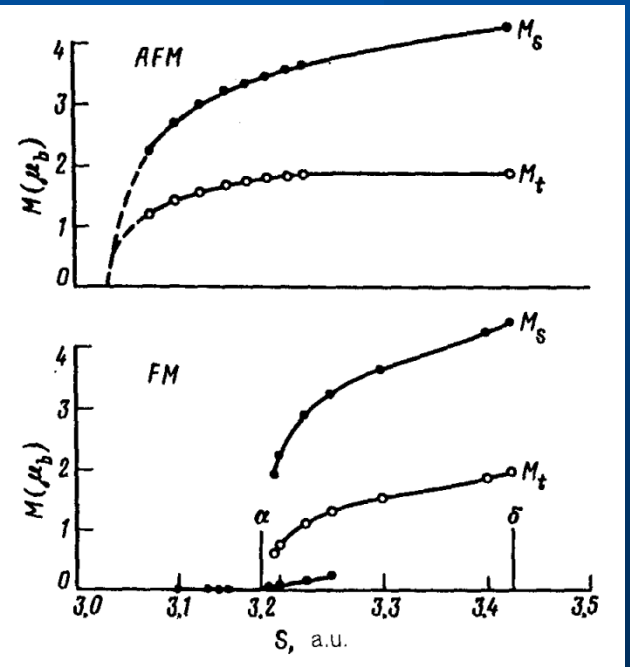

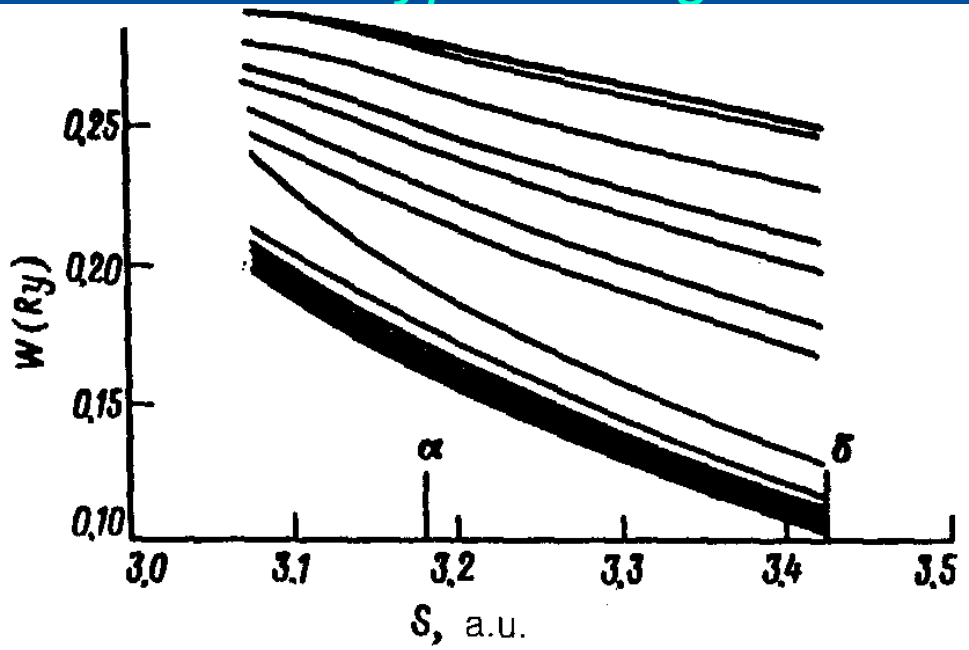

Elemental Pu III

Correlated electrons in δ-plutonium within a dynamical mean-field picture

S. Y. Savrasov, G. Kotliar & E. Abrahams

NATURE | VOL 410 | 12 APRIL 2001

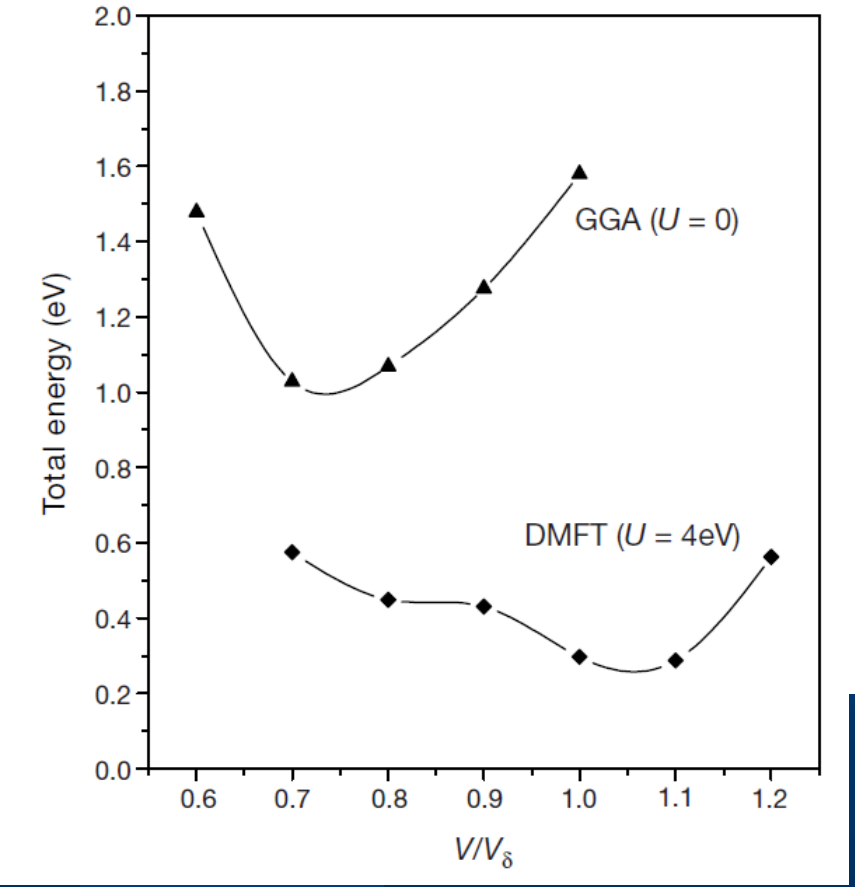

PHYSICAL REVIEW B 67, 235105 (2003)

Modeling the actinides with disordered local moments

Anders M. N. Niklasson,[1] John M. Wills,[1] Mikhail I. Katsnelson,[2,3] Igor A. Abrikosov,[3] Olle Eriksson,[3] and Börje Johansson[3,4]

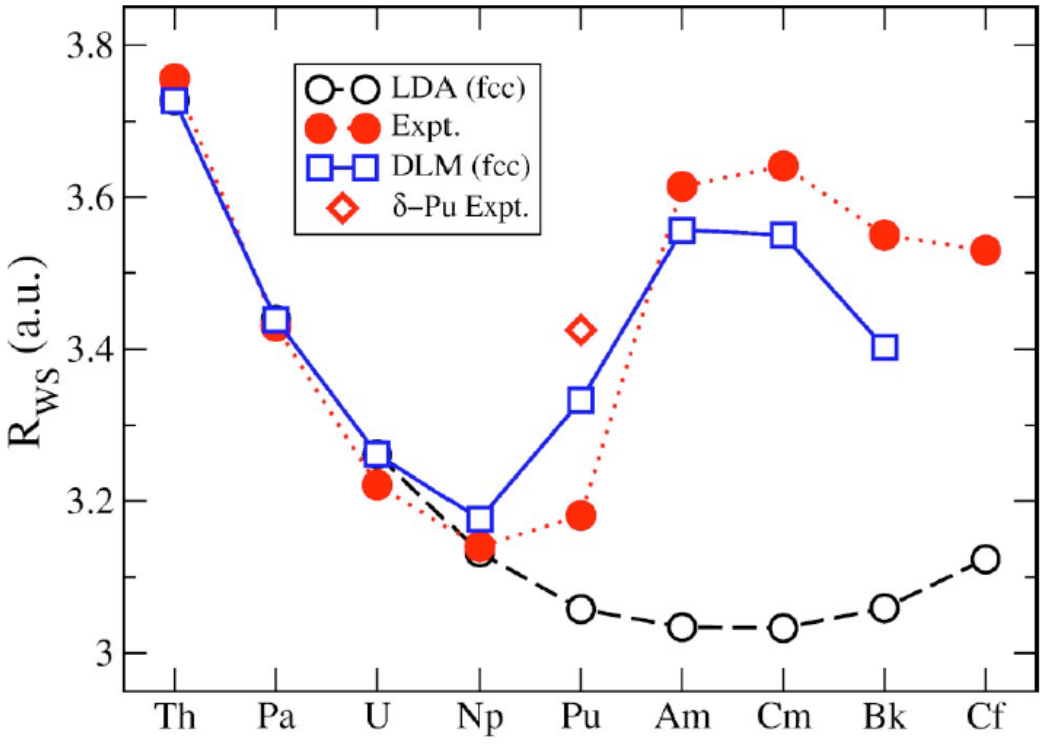

Local moments would help, but...

Is Pu magnetic?

PHYSICAL REVIEW B **72**, 054416 (2005)

Absence of magnetic moments in plutonium

J. C. Lashley,[1] A. Lawson,[1] R. J. McQueeney,[2] and G. H. Lander[3]

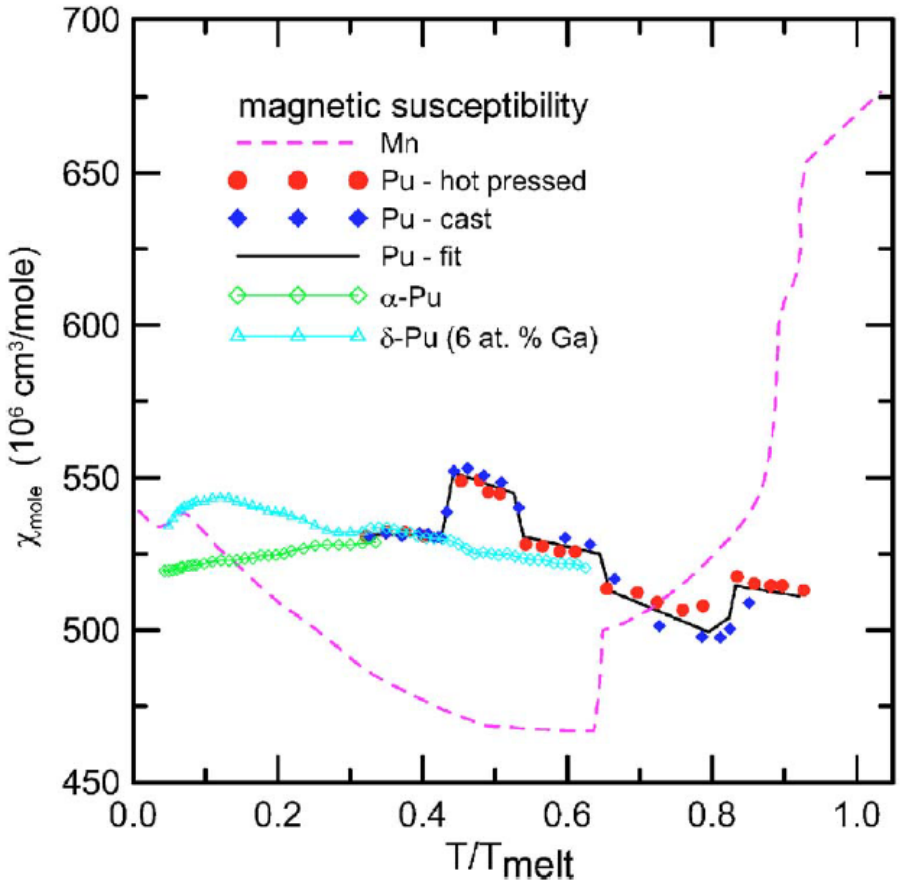

Direct evidences from neutron scattering: no magnetic moments, neither ordered nor disordered, neither spin nor orbital

Hypothesis: basic $5f^6$ configuration like in Am (S=3, L=3, J=L-S=0)

Shick, Drchal, Havela, EPL 69, 588 (2005); Pourovskii, MIK, Lichtenstein, Havela, Gouder, Wastin, Shick, Drchal, Lander, EPL 74, 479 (2006).

Problems with the data of core-level spectroscopy and heat capacity

“Racah materials”

PHYSICAL REVIEW B 87, 020505(R) (2013)

Unified character of correlation effects in unconventional Pu-based superconductors and δ-Pu

A. B. Shick,[1,2] J. Kolorenc,[2] J. Rusz,[2,3] P. M. Oppeneer,[3] A. I. Lichtenstein,[4] M. I. Katsnelson,[5] and R. Caciuffo[1]

LDA+DMFT

SCIENTIFIC REPORTS | 5:15429 |

Racah materials: role of atomic multiplets in intermediate valence systems

A. B. Shick[1], L. Havela[2], A. I. Lichtenstein[3,4] & M. I. Katsnelson[4,5]

Calculations for δ-Pu vs PES

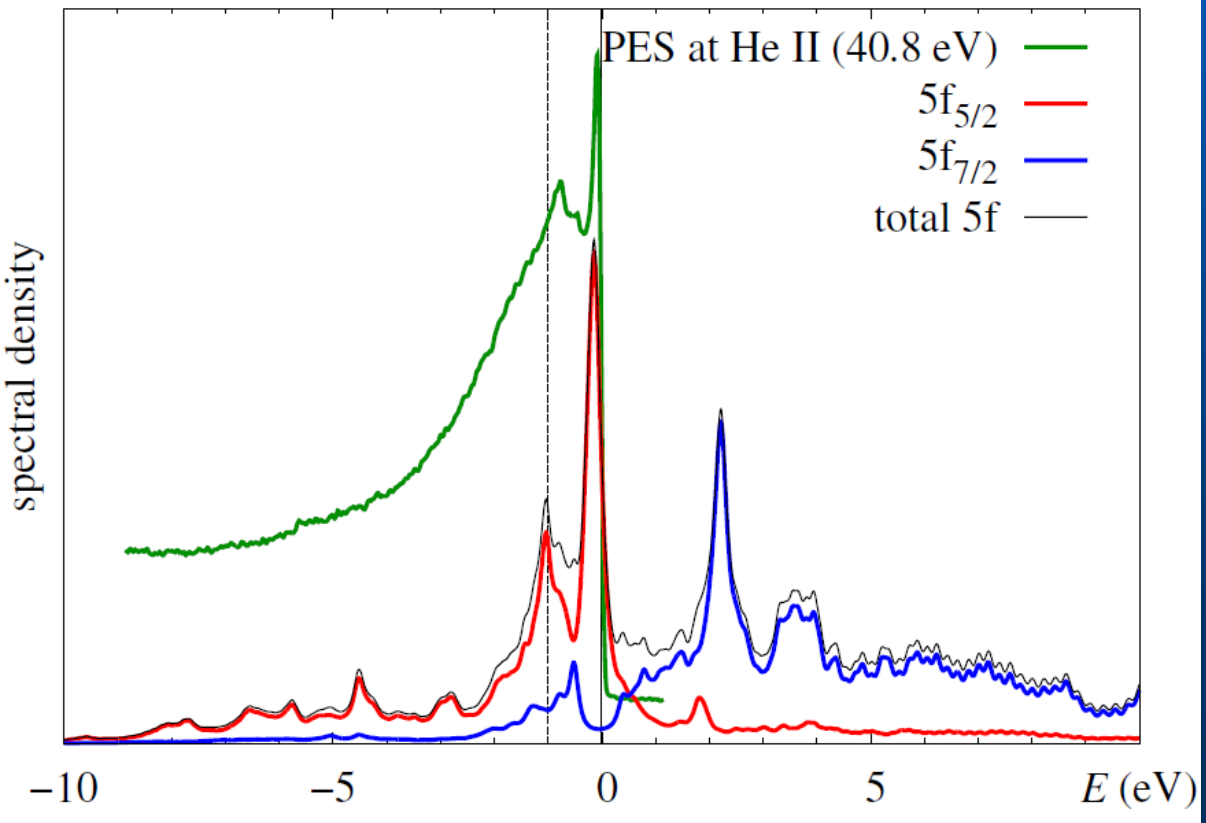

Peak at E_f is not ”Kondo” but due to f^6-to-f^5 multiplet transition

Three peak structure: f^6-to-f^5 multiplet transitions are better resolved than f^5-to-f^4 transitions.

Racah materials II

We see multiplets $f^6 \rightarrow f^5$ but not $f^5 \rightarrow f^4$
Configuration is close to f^5 – good; nonmagnetic since mixed-valent – good; but many-body effects are due to the mixture of f^6 configuration

$$a^{\dagger}_{il\sigma m} = (n+1)^{1/2} \sum G^{S'L'}_{SL} C^{L'\mu'}_{L\mu,lm} C^{S'M'}_{SM,\frac{1}{2}\sigma} X_i(S'L'M'\mu', SLM\mu)$$

$G^{S'L'}_{SL}$ *fractional parentage coefficients*

$X_i(\alpha\beta) = |i\alpha\rangle\langle i\beta|$ *Hubbard X-operators*

$$X_i(\alpha\beta)X_i(\gamma\varepsilon) = \delta_{\beta\gamma}X_i(\alpha\varepsilon), \sum_{\alpha} X_i(\alpha\alpha) = 1$$

Why δ-Pu is non-magnetic?

f-shell n_f=5.2:
80% [f^5] + 20% [f^6]
Intermediate valence

Coulomb interaction between f- and d-states responsible for valence fluctuations

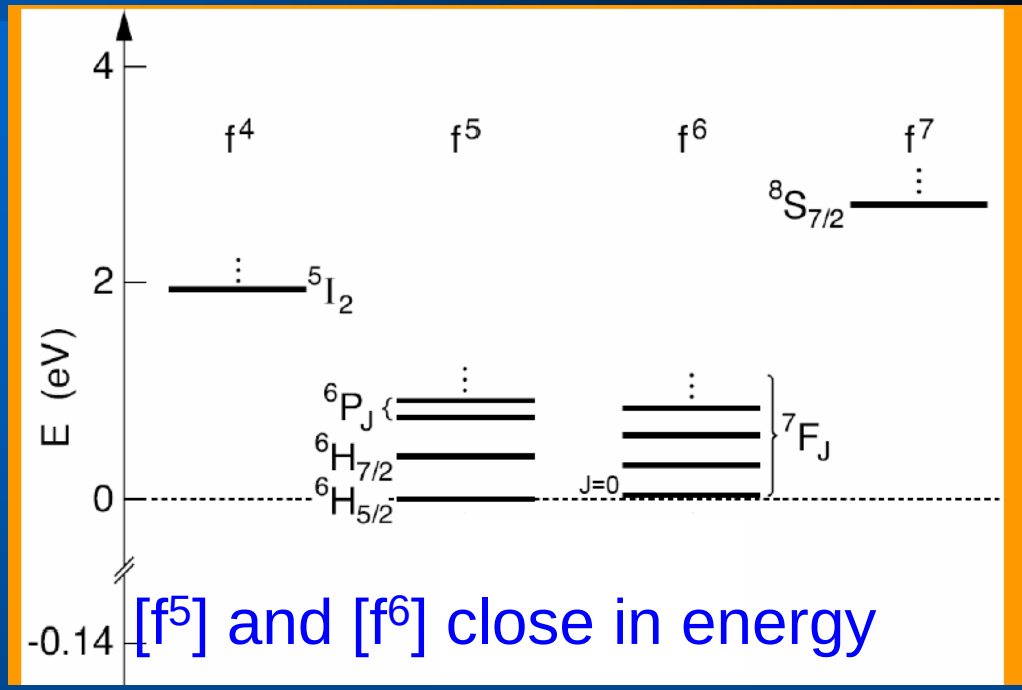

When there is a mixing of magnetic [f^n] and non-magnetic [f^{n+1}] multiplets the resulting state is non-magnetic.

Not a “theorem”, depends on hybridization parameters!

4f Mixed Valence Compounds

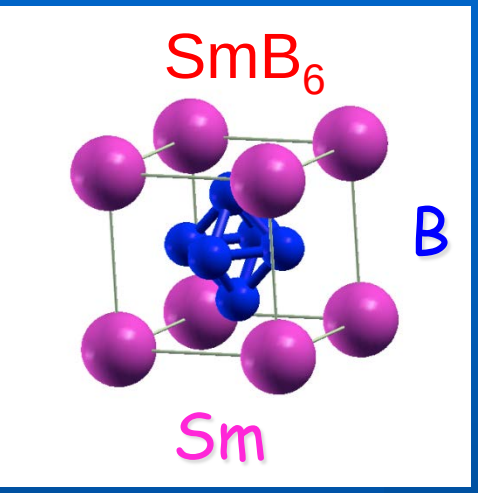

Narrow-gap semiconductor
Topological insulator
Nonmagnetic

LDA+DMFT results

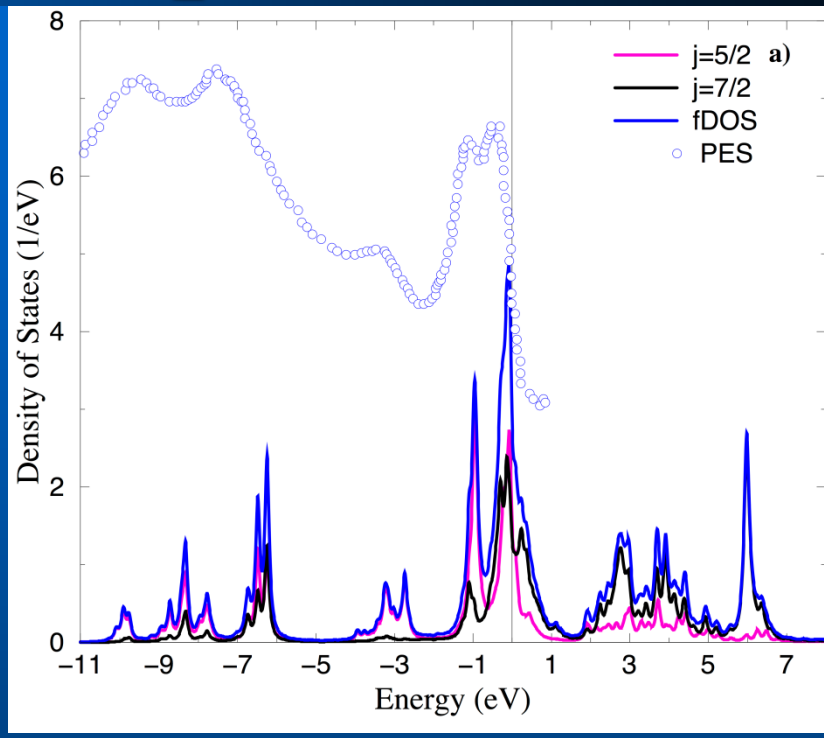

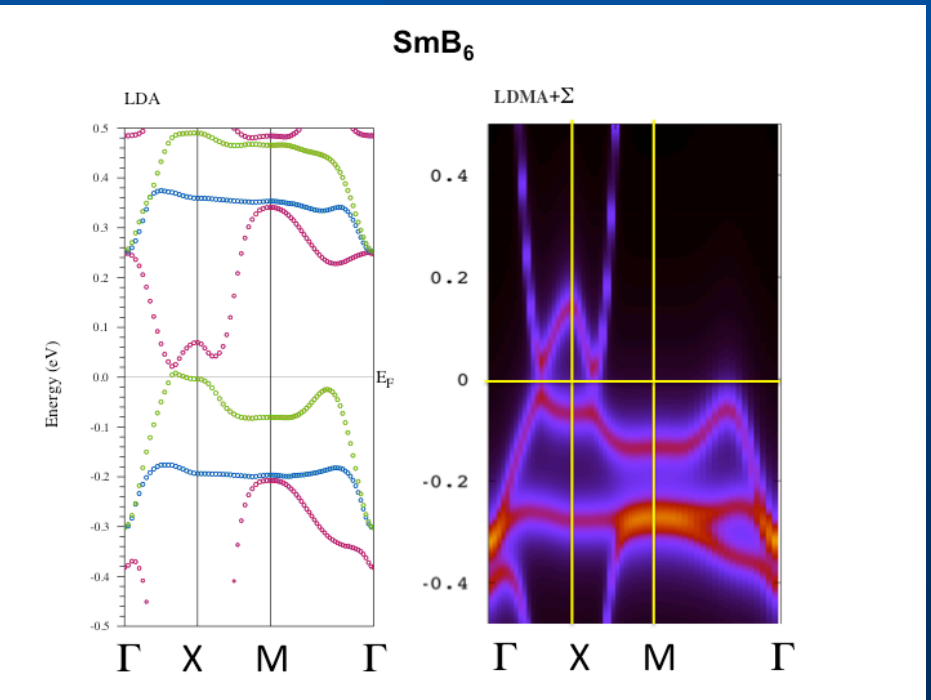

We see multiplets $f^6 \rightarrow f^5$ but not $f^5 \rightarrow f^4$ – "Racah material"

Contrary to the case of TmSe

Part II: Graphene as CERN on the desk

Allotropes of Carbon

Diamond, Graphite

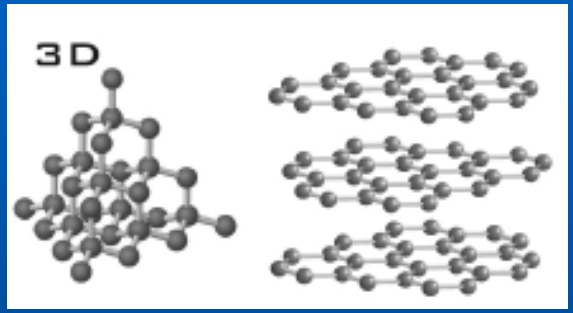

Graphene: prototype
truly 2D crystal

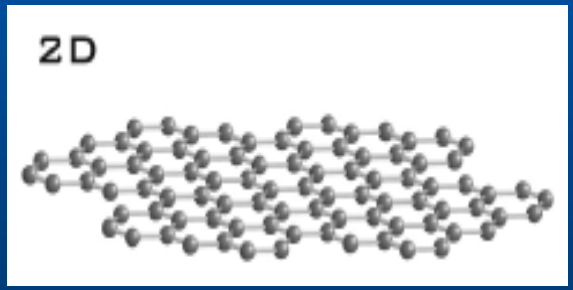

Nanotubes

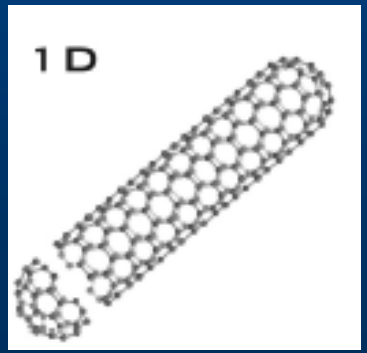

Fullerenes

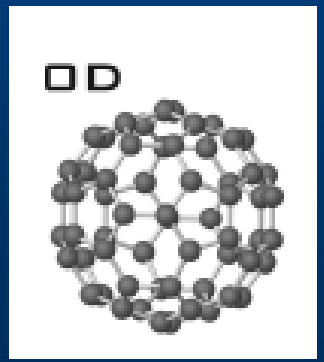

Massless Dirac fermions

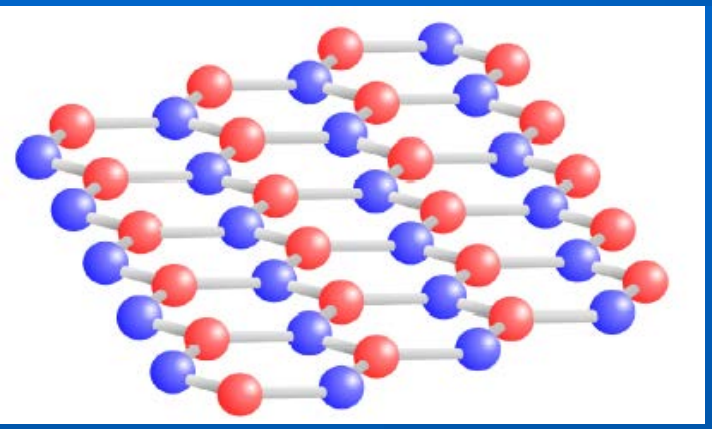

Pseudospin:
Sublattice A ↑
Sublattice B ↓

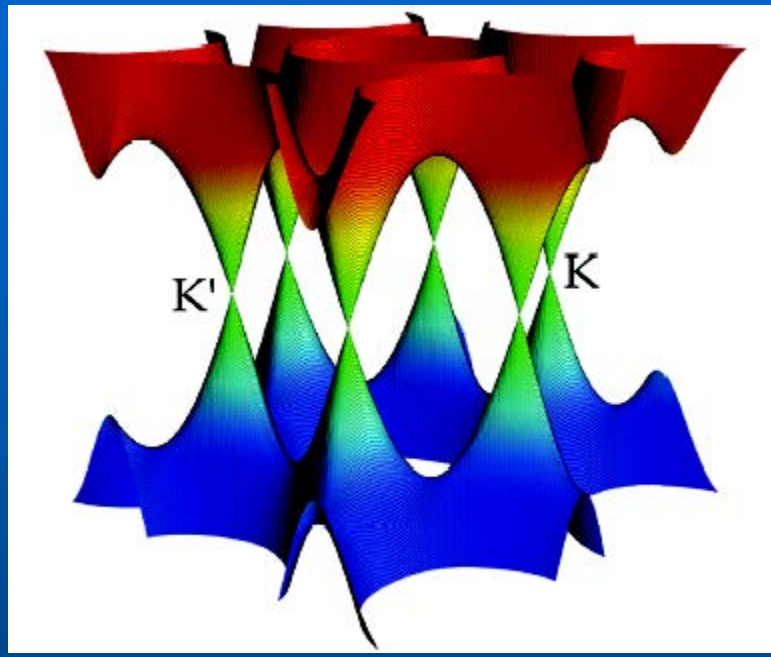

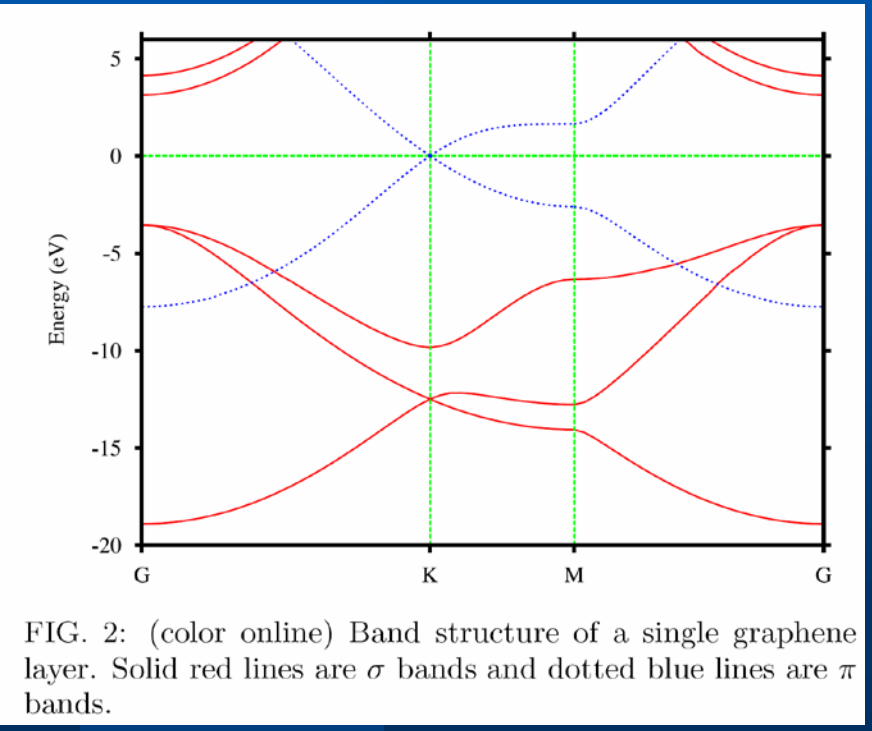

FIG. 2: (color online) Band structure of a single graphene layer. Solid red lines are σ bands and dotted blue lines are π bands.

sp^2 hybridization, π bands crossing the neutrality point

Neglecting intervalley scattering: massless Dirac fermions

Symmetry protected (*T* and *I*)

Massless Dirac fermions II

Spectrum near *K* (*K'*) points is linear.
Conical cross-points: provided by symmetry and thus robust property

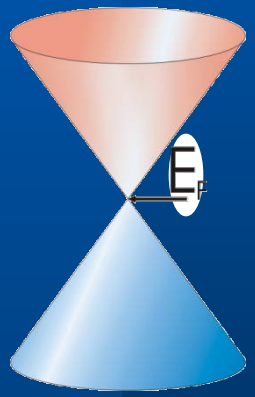

Undoped

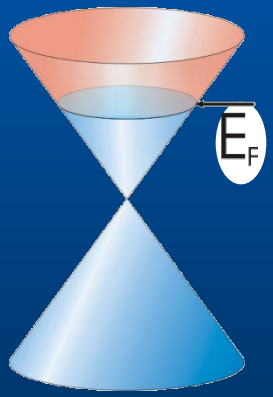

Electron

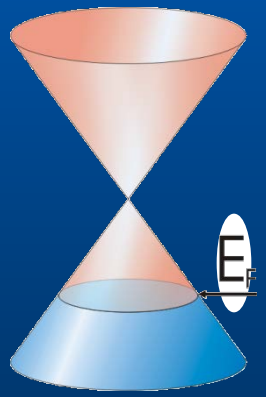

Hole

Massless Dirac fermions in condensed matter physics

1. d-wave superconductors
2. Vortices in superconductors and in superfluid helium-3
3. Topological insulators
4. Graphene

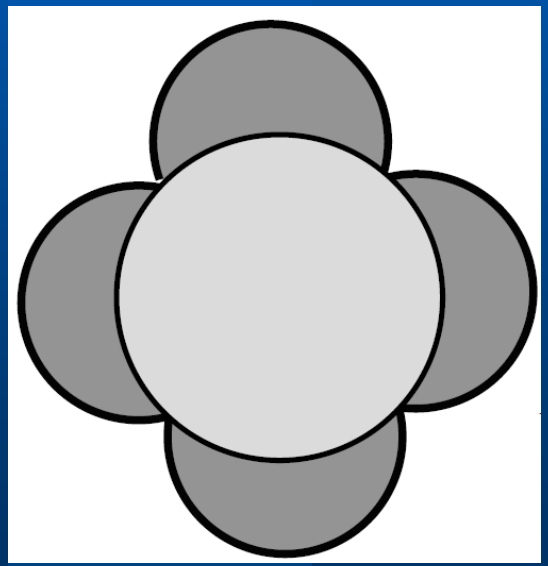

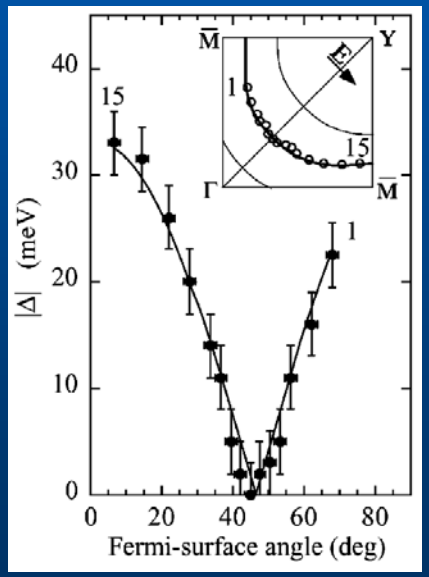

Gap in high-Tc cuprates

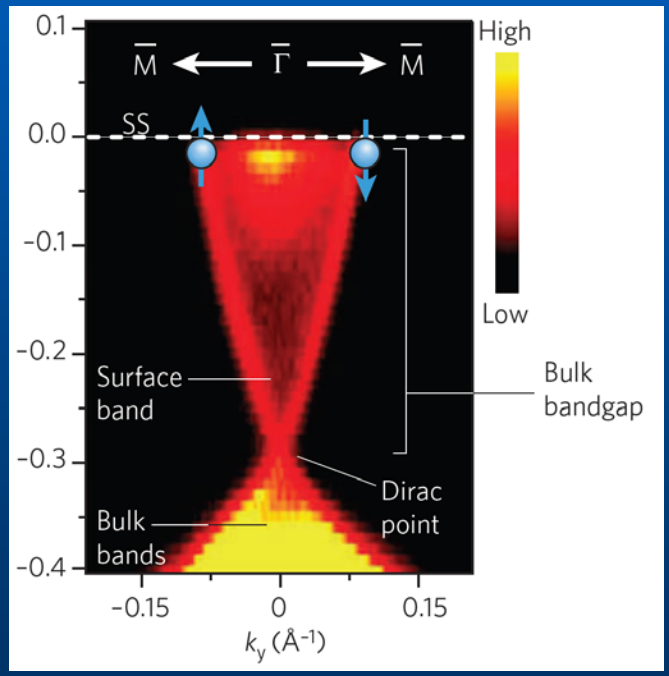

Electronic structure on surface of Bi_2Se_3

Chiral tunneling and Klein paradox

MIK, Novoselov, Geim, Nat. Phys. 2, 620 (2006)

Electronics: heterostructures (*p-n-p* junctions etc.)

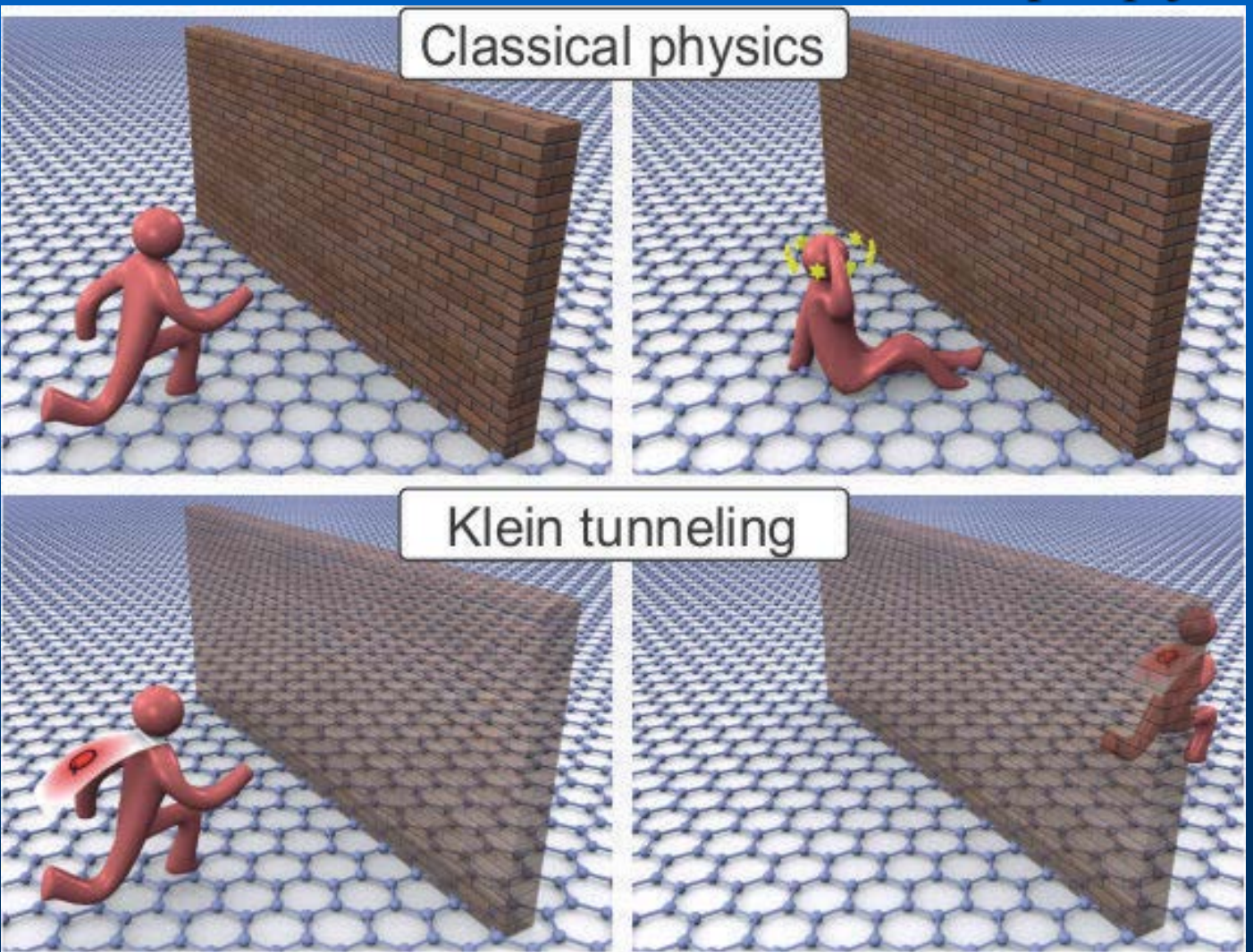

(C) Florian Sterl

Klein paradox II

Ultrarelativisic

Nonrelativistic

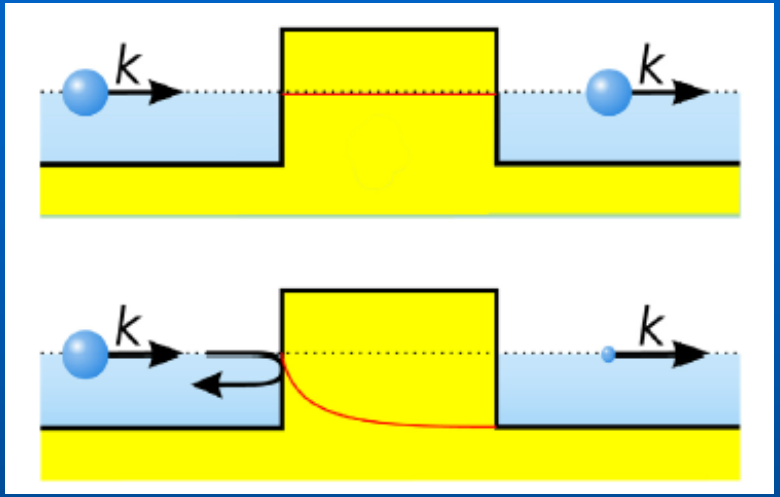

Tunnel effect: momentum and coordinate are complementary variables, kinetic and potential energy are not measurable simultaneously

Relativistic case: even the *coordinate itself* is not measurable, particle-antiparticle pair creation

Klein paradox III

Transmission probability

Barrier width 100 *nm*

Electron concentration outside barrier 0.5×10^{12} cm^{-2}

Hole concentration inside barrier 1×10^{12} cm^{-2} (red) and 3×10^{12} cm^{-2} (blue)

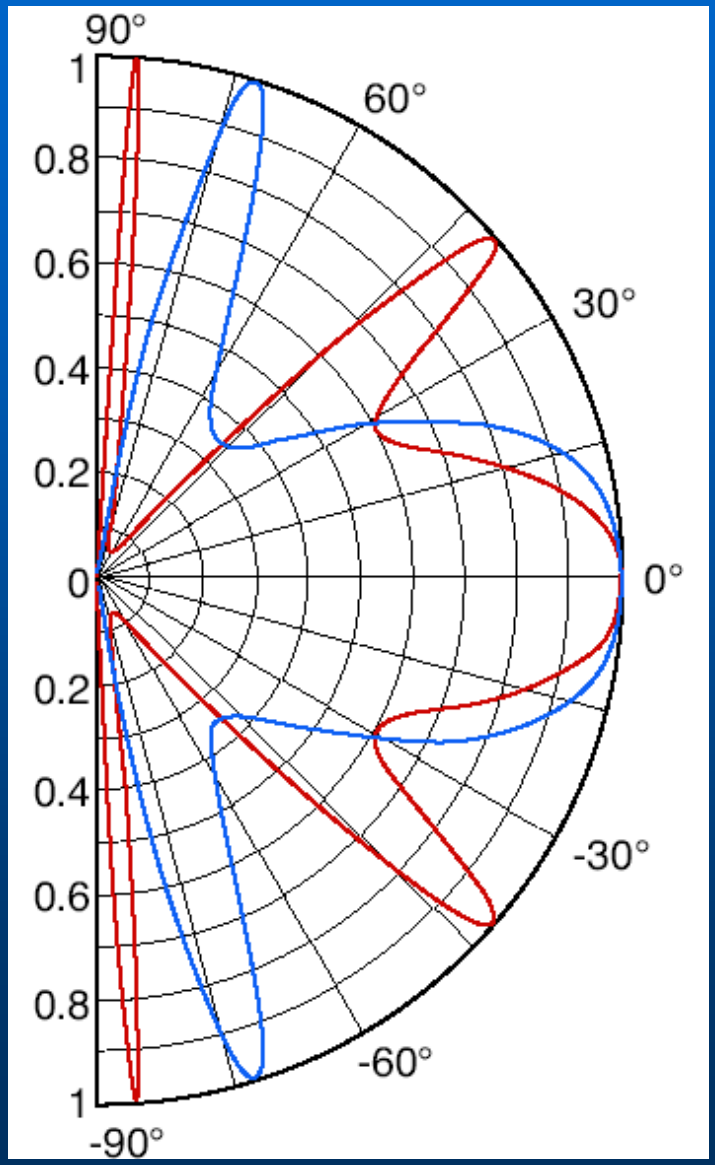

Klein tunneling: Experimental confirmation

PRL **102,** 026807 (2009) PHYSICAL REVIEW LETTERS week ending 16 JANUARY 2009

Evidence for Klein Tunneling in Graphene *p-n* Junctions

N. Stander, B. Huard, and D. Goldhaber-Gordon*

Department of Physics, Stanford University, Stanford, California 94305, USA

(Received 13 June 2008; published 16 January 2009)

Transport through potential barriers in graphene is investigated using a set of metallic gates capacitively coupled to graphene to modulate the potential landscape. When a gate-induced potential step is steep enough, disorder becomes less important and the resistance across the step is in quantitative agreement with predictions of Klein tunneling of Dirac fermions up to a small correction. We also perform magnetoresistance measurements at low magnetic fields and compare them to recent predictions.

nature physics

LETTERS

PUBLISHED ONLINE: 1 FEBRUARY 2009 | DOI: 10.1038/NPHYS1198

Quantum interference and Klein tunnelling in graphene heterojunctions

Andrea F. Young and Philip Kim*

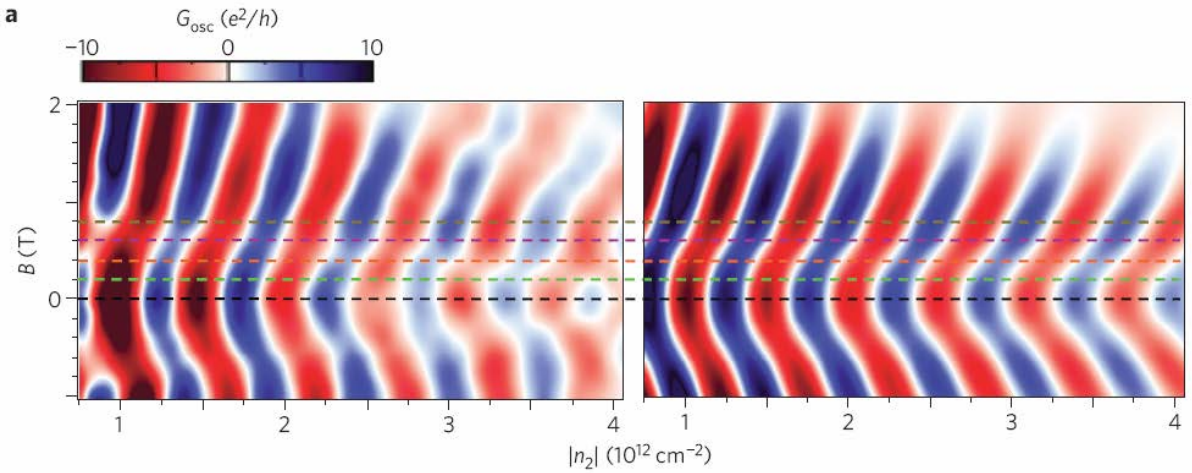

Klein tunneling prevents localization

Back scattering is forbidden for chiral fermions! Magic angle = 0

Nonuniversal magic angle for bilayer exists!

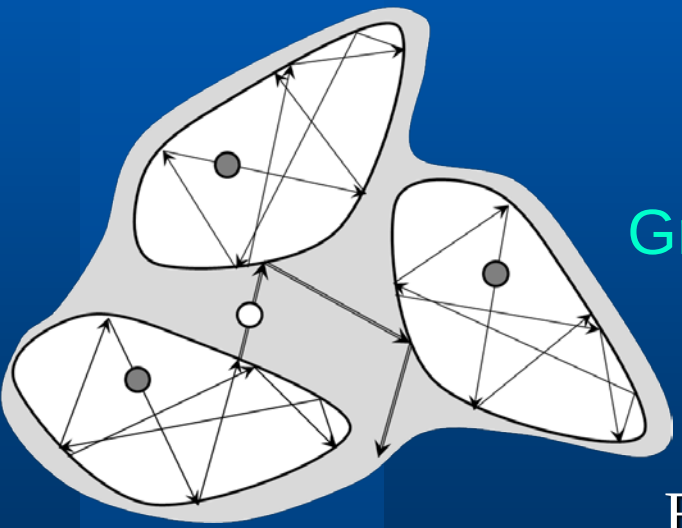

Graphene

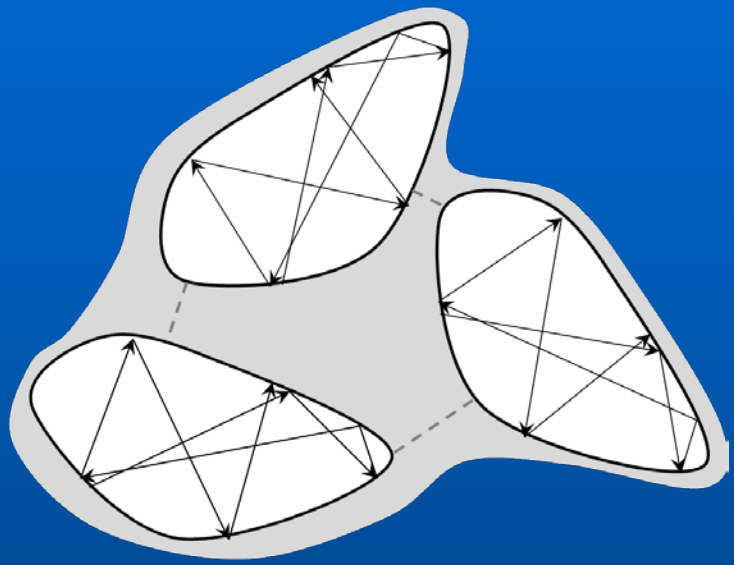

Conventional semiconductors

Electrons cannot be locked by random potential relief neither for single-layer nor for bilayer graphene – absence of localization and minimal conductivity?!

Inhomogeneities are unavoidable

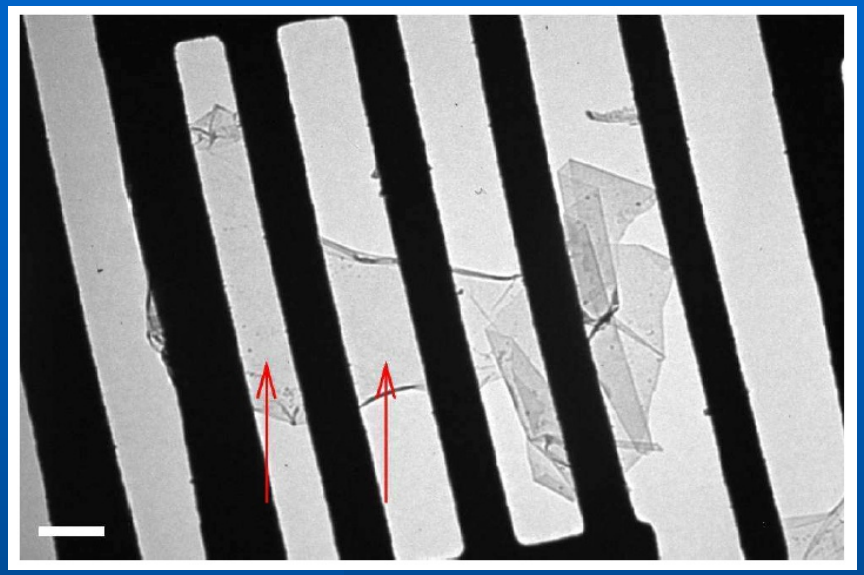

Freely suspended graphene membrane is corrugated

Meyer et al, *Nature 446, 60 (2007)*

2D crystals in 3D space cannot be flat, due to bending instability

Atomistic simulations of intrinsic ripples

Fasolino, Los & MIK, Nature Mater. 6, 858 (2007)

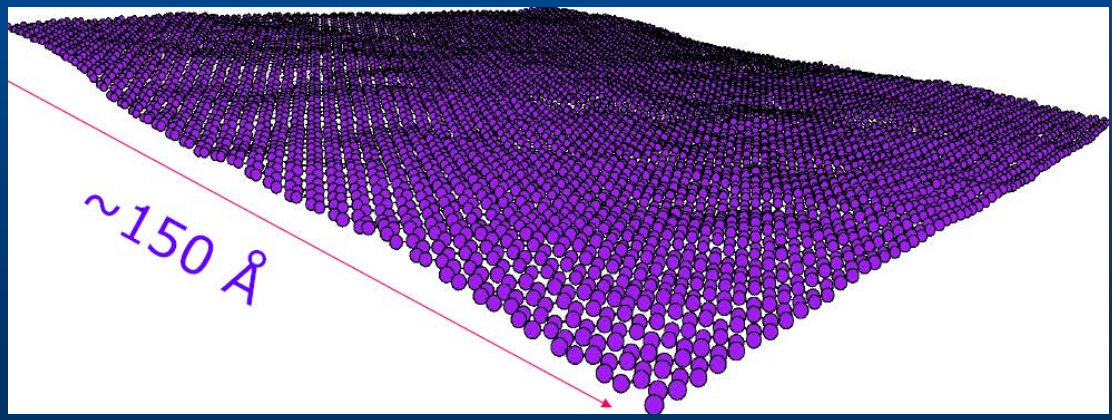

Ripples and puddles

Gibertini, Tomadin, Polini, Fasolino & MIK, PR B 81, 125437 (2010)

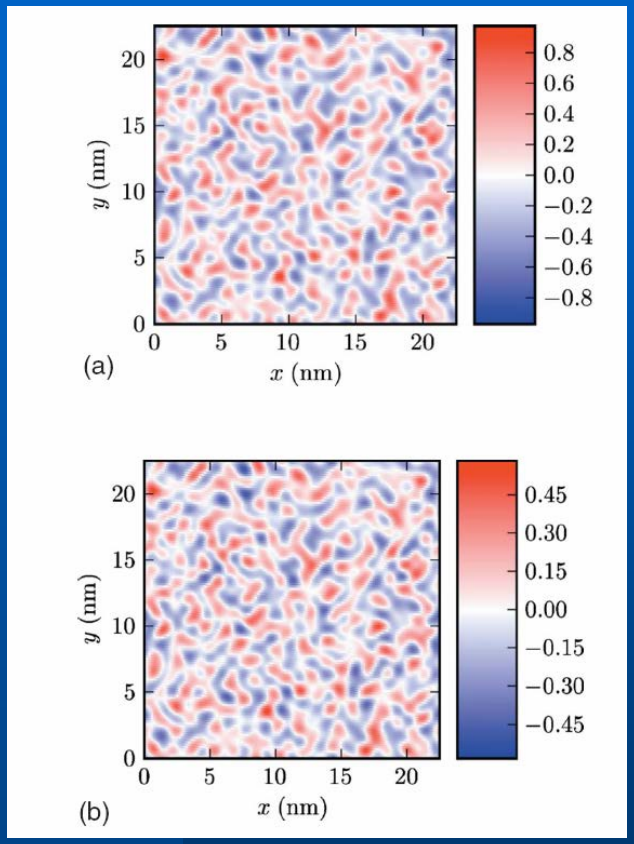

FIG. 4. (Color online) Top panel: fully self-consistent electronic density profile $\delta n(\boldsymbol{r})$ (in units of 10^{12} cm^{-2}) in a corrugated graphene sheet. The data reported in this figure have been obtained by setting $g_1=3$ eV, $\alpha_{ee}=0.9$ (this value of α_{ee} is the commonly used value for a graphene sheet on a SiO_2 substrate), and an average carrier density $\bar{n}_c \simeq 0.8\times10^{12}$ cm^{-2}. Bottom panel: same as in the top panel but for $\alpha_{ee}=2.2$ (this value of α_{ee} corresponds to suspended graphene).

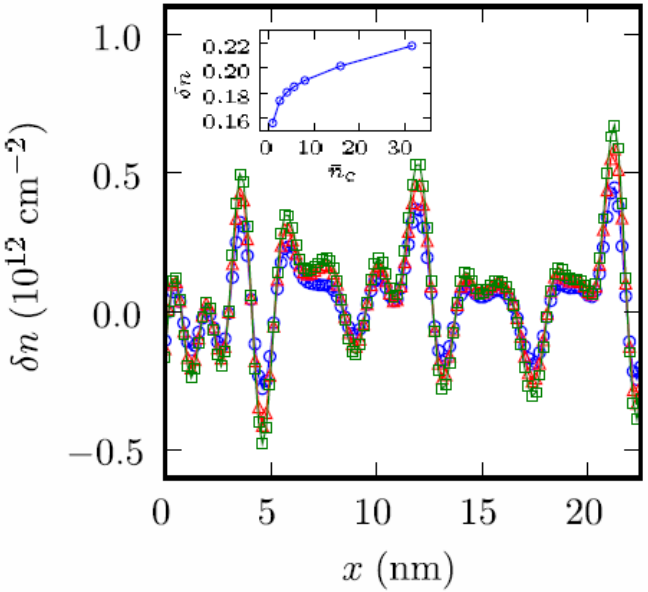

FIG. 9. (Color online) One-dimensional plots of the self-consistent density profiles (as functions of x in nm for $y=21.1$ nm) for different values of doping: $\bar{n}_c \simeq 0.8\times10^{12}$ cm^{-2} (circles), $\bar{n}_c \simeq 3.96\times10^{12}$ cm^{-2} (triangles), and $\bar{n}_c \simeq 3.17\times10^{13}$ cm^{-2} (squares). The data reported in this figure have been obtained by setting $g_1=3$ eV and $\alpha_{ee}=2.2$. The inset shows $\delta n(\boldsymbol{r})$ (in units of 10^{12} cm^{-2}) at a given point $\boldsymbol{r}$ in space as a function of the average carrier density $\bar{n}_c$ (in units of 10^{12} cm^{-2}).

Ripples and puddles II

Graphene on SiO_2

Gibertini, Tomadin, Guinea, MIK & Polini PR B 85, 201405 (2012)

Experimental STM data: V.Geringer et al (M.Morgenstern group)

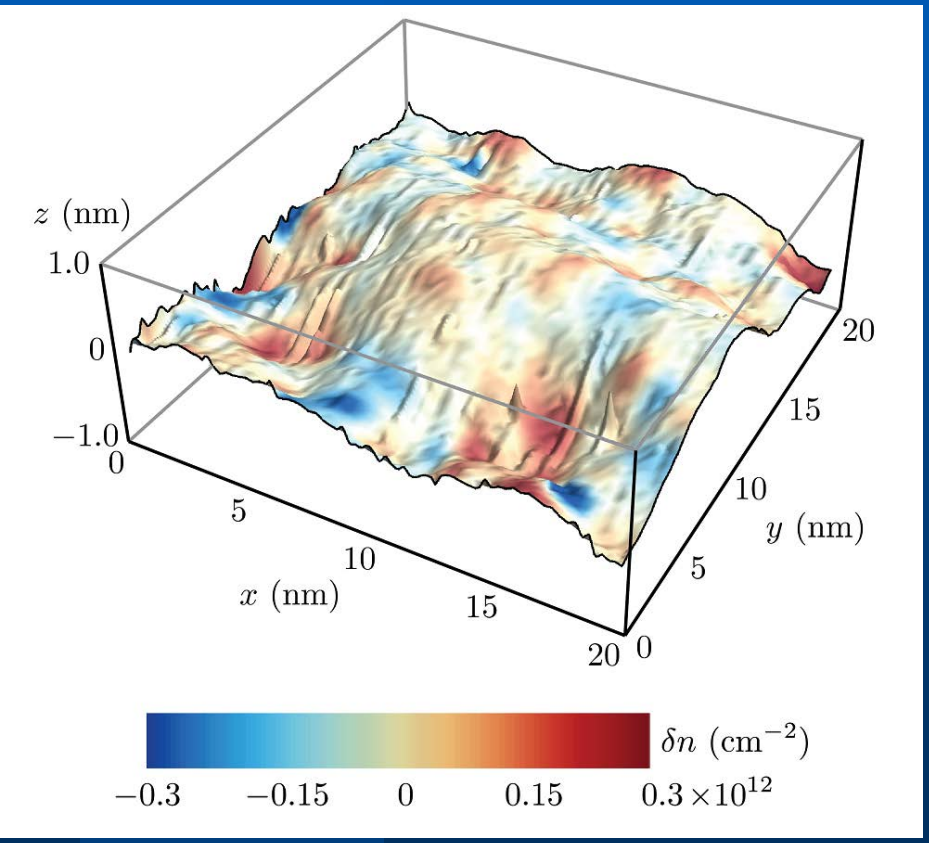

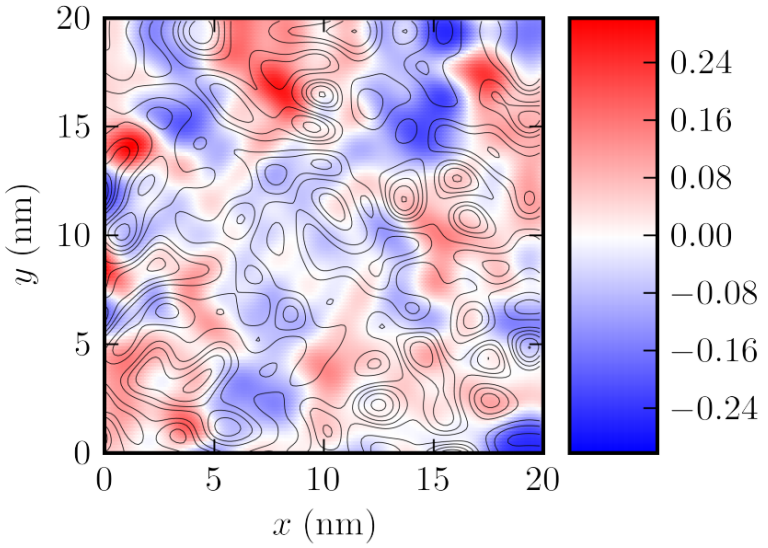

FIG. 3: (Color online) Fully self-consistent induced carrier-density profile $\delta n(\boldsymbol{r})$ (in units of 10^{12} cm^{-2}) in the corrugated graphene sheet shown in Fig. 1. The data reported in this figure have been obtained by setting $g_1 = 3$ eV, $\alpha_{ee} = 0.9$, and an average carrier density $\bar{n}_c \approx 2.5 \times 10^{11}$ cm^{-2}. The thin solid lines are contour plots of the curvature $\nabla^2_{\boldsymbol{r}} h(\boldsymbol{r})$. Note that there is no simple correspondence between topographic out-of-plane corrugations and carrier-density inhomogeneity.

The role of Klein tunneling

Without Klein tunneling graphene near the neutrality point will be insulator and, anyway, will have a high enough mobility

At the same time: a problem with transistors, one needs to use a complicated and indirect ways

Crucial phenomenon for physics and electronic applications of graphene

Field-Effect Tunneling Transistor Based on Vertical Graphene Heterostructures
L. Britnell, *et al.*
Science **335**, 947 (2012);

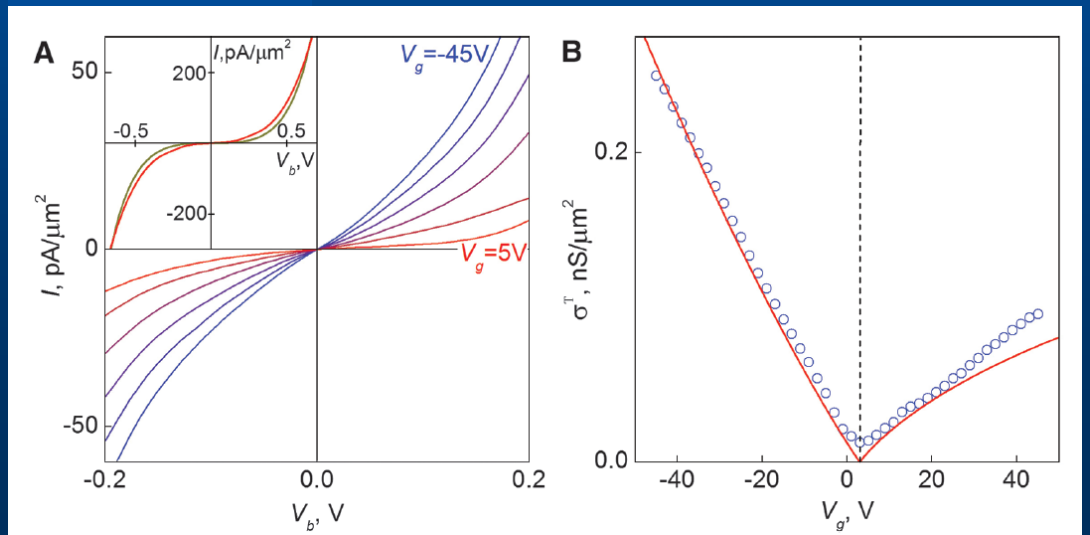

Tunneling transistor with vertical geometry

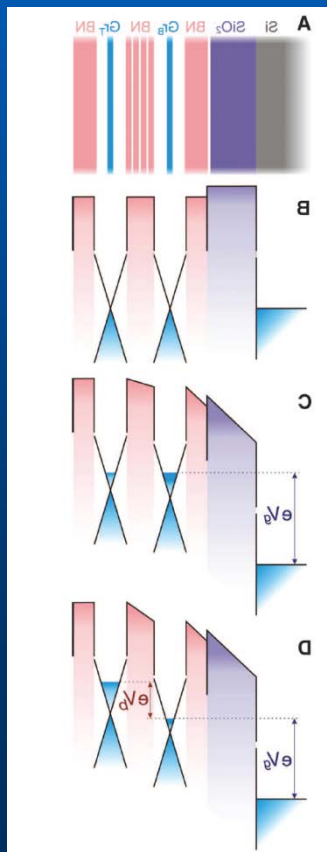

Relativistic collapse for supercritical charges

Coulomb potential

$$V_0(\mathbf{r}) = \frac{Ze^2}{\epsilon r}$$

following Shytov, MIK & Levitov, PRL 99, 236801; 246803 (2007)

Naive arguments: Radius of atom *R*, momentum *ħ/R*. Nonrelativistic case:

E(R) ~ ħ² /mR² – Ze²/R

Minimum gives a size of atom.

Relativistic case: *E(R) ~ ħc*/R – Ze²/R*

Either no bound state or fall on the center.

Vacuum reconstruction at *Z* > 170

Supercritical charges II

Superheavy nuclei

I. Pomeranchuk and Y. Smorodinsky, J. Phys. USSR **9**, 97 (1945)

Graphene:
$v \approx c/300$,
$\alpha_{eff} \approx 1$

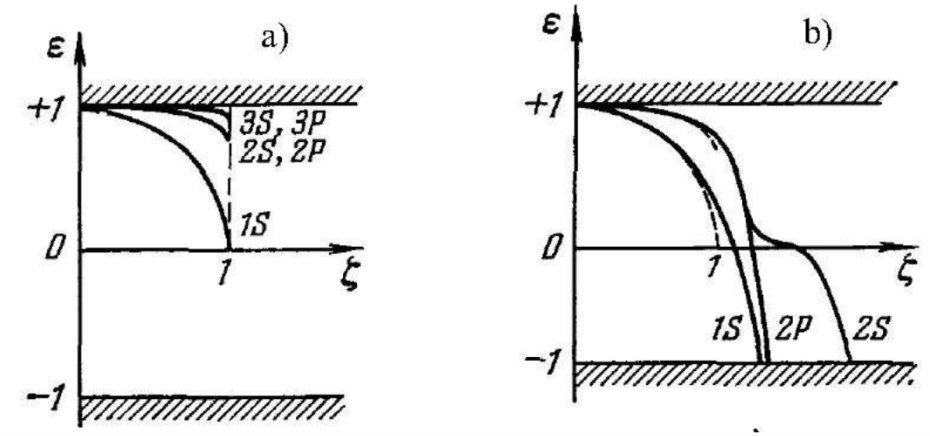

FIG. 1: a) Energy levels of superheavy atoms obtained from Dirac equation for Coulomb potential $-Ze^2/r$, plotted as a function of $\zeta = Z\alpha$, where Z is nuclear charge, and $\alpha = e^2/\hbar c$ is the fine structure constant. Energy is in the units of mc^2. (b) Energy levels for Coulomb potential regularized on the nuclear radius. As Z increases, the discrete levels approach the continuum of negative-energy states and dive into it one by one at supercritical $Z > 170$ (from Ref.[23]).

[23] Y. B. Zeldovich and V. S. Popov, Usp. Fiz. Nauk **105**, 403

Supercritical charges III

$\beta = Ze^2/\hbar v_F \varepsilon > ½$

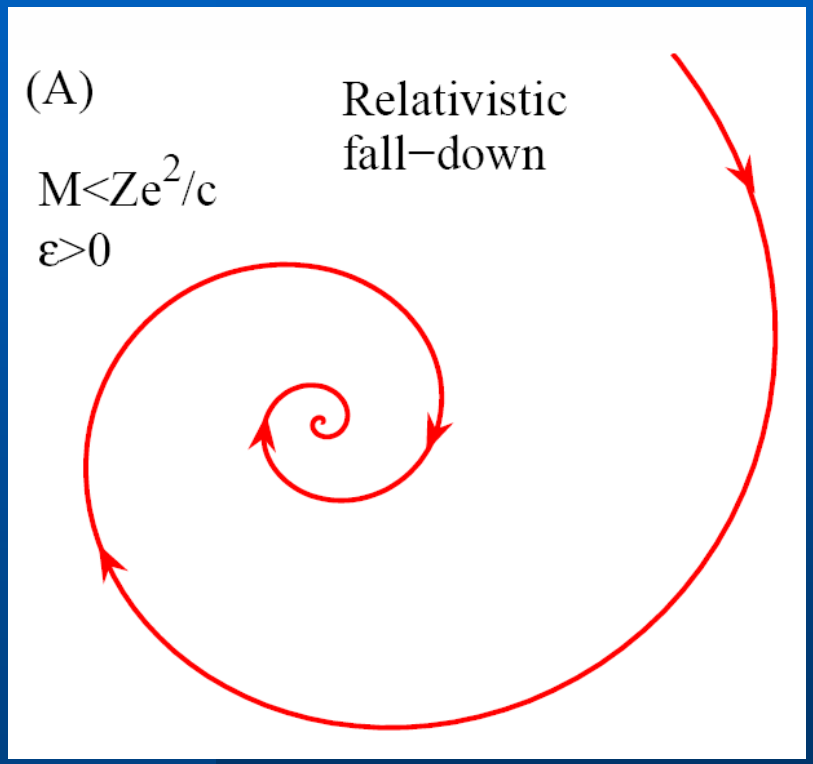

Quasi-local states

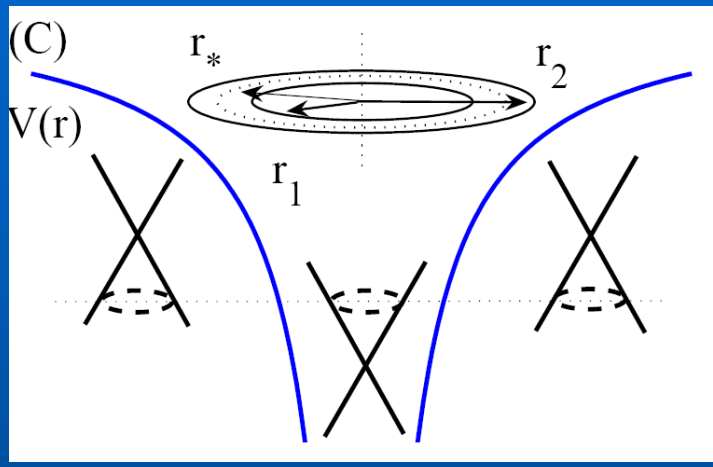

Klein tunneling

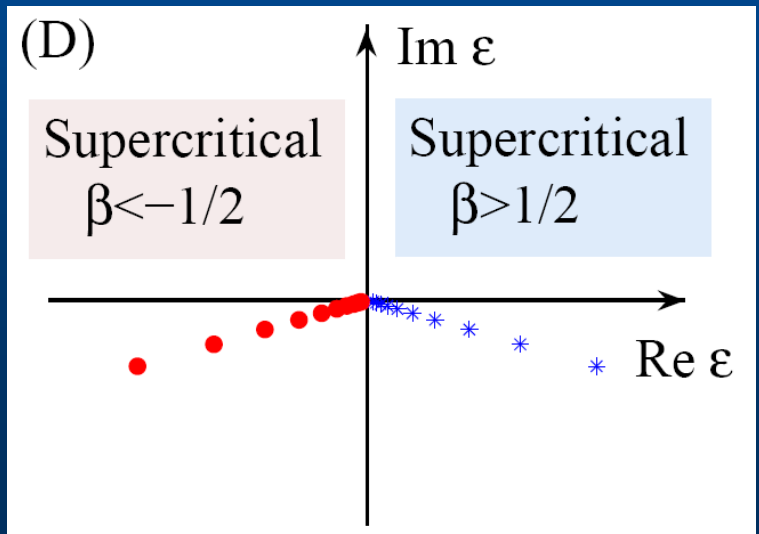

Supercritical charge IV

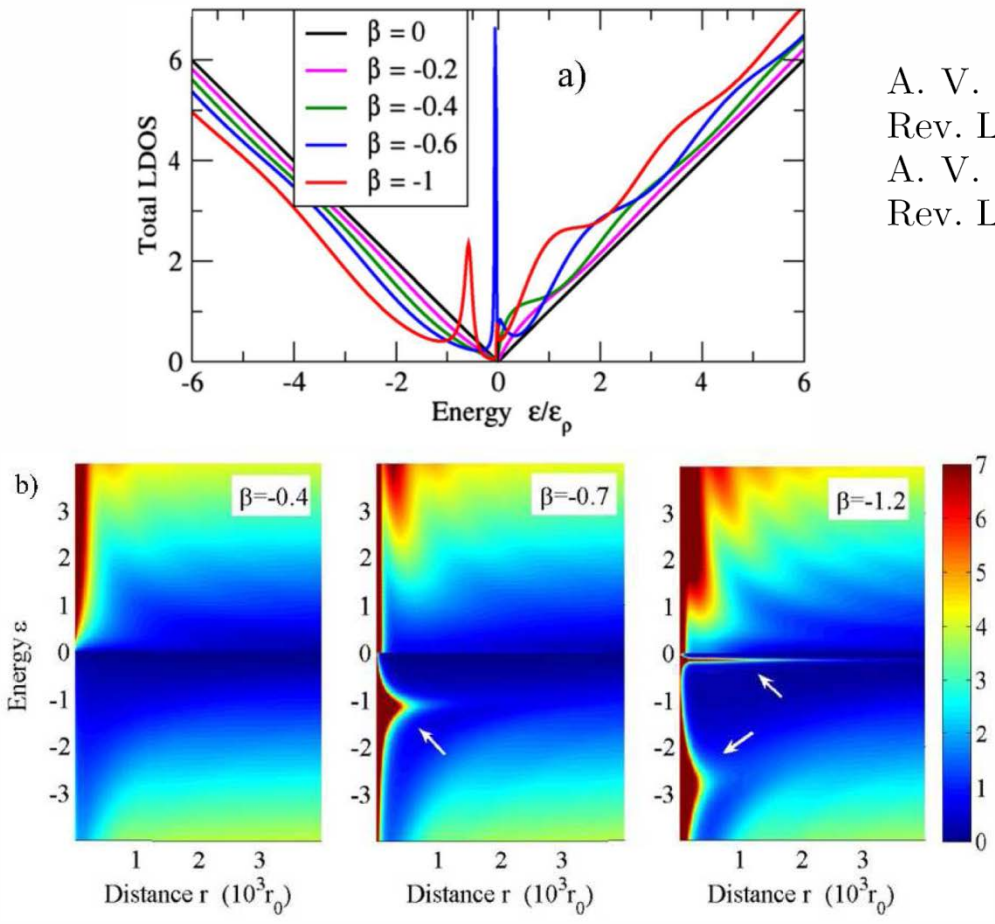

A. V. Shytov, M. I. Katsnelson, and L. S. Levitov, Phys. Rev. Lett. **99**, 236801 (2007), arXiv:0705.4663

A. V. Shytov, M. I. Katsnelson, and L. S. Levitov, Phys. Rev. Lett. **99**, 246802 (2007), arxiv.org:0708.0837

FIG. 3: (a) Local density of states (12) calculated at a fixed distance $\rho = 10^3 r_0$ from the charged impurity, where r_0 is a short-distance parameter of the order of carbon lattice spacing (from Ref.[10]). Peaks in the LDOS, which appear at supercritical β and move to more negative energies at increasing $|\beta|$, correspond to the resonant states. (b) Spatial map of the density of states, shown for several values of β, with resonances marked by white arrows (from Ref.[11]). Note that the spatial width of the resonances decreases at they move to lower energies, $\Delta\rho \propto 1/|\varepsilon|$, while the linewidth increases, $\gamma \propto |\varepsilon|$. The oscillatory structure at positive energies represents standing waves with maxima at $k\rho \approx (n + \frac{1}{2})\pi$, similar to those studied in carbon nanotubes [26]. Energy is given in the units of $\varepsilon_0 = 10^{-3}\hbar v/r_0 \approx 30\,\mathrm{mV}$ for $r_0 = 0.2\,\mathrm{nm}$.

Exper.: Tuning Z by Building Artificial Nuclei from Ca Dimers

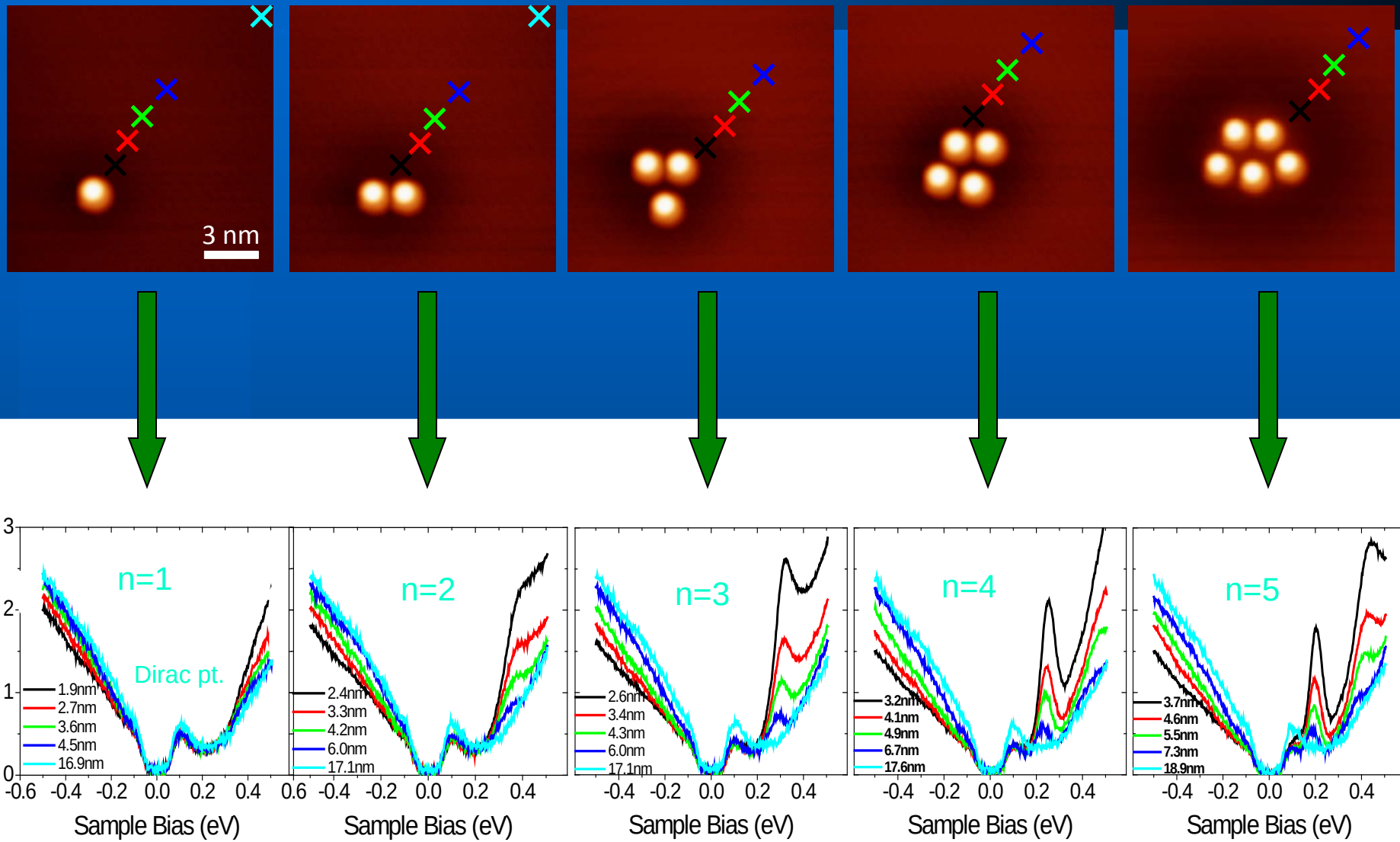

Y. Wang et al, Science 340, 734 (2013)

Pseudomagnetic fields

Nearest-neighbour approximation: changes of hopping integrals

$$\gamma = \gamma_0 + \left(\frac{\partial\gamma}{\partial\overline{u}_{ij}}\right)_0 \overline{u}_{ij}$$

$$H = v_F\sigma\left(-i\hbar\nabla - \frac{e}{c}\mathcal{A}\right)$$

"Vector potentials"

$$\mathcal{A}_x = \frac{c}{2ev_F}\left(\gamma_2 + \gamma_3 - 2\gamma_1\right),$$

$$\mathcal{A}_y = \frac{\sqrt{3}c}{2ev_F}\left(\gamma_3 - \gamma_2\right),$$

K and *K'* points are shifted in opposite directions; Umklapp processes restore time-reversal symmetry

Review: M. Vozmediano, MIK & F. Guinea, Phys. Rep. 496, 109 (2010)

Psedomagnetic fields II

Within elasticity theory (continuum limit)

$$\mathbf{A} = \frac{\beta}{a}\begin{pmatrix} u_{xx} - u_{yy} \\ -2u_{xy} \end{pmatrix}$$

$$\beta = -\partial \ln t / \partial \ln a \approx 2$$

Pseudomagnetic field

Shear deformations create vector potential

$$B_S = \frac{\partial A_y}{\partial x} - \frac{\partial A_x}{\partial y} = \frac{1}{r}\frac{\partial A_r}{\partial \theta} - \frac{\partial A_\theta}{\partial r} - \frac{A_\theta}{r}$$

Dilatation creates scalar (electrostatic) potential

$$V_1 = g_1(u_{xx} + u_{yy})$$

Gauge fields from mechanics: back to Maxwell

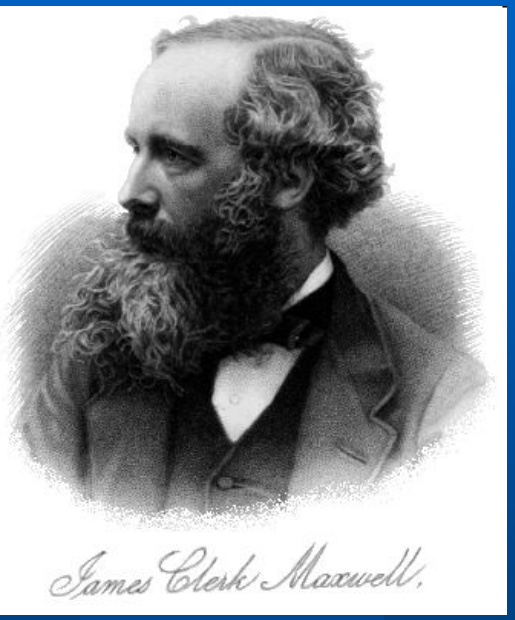

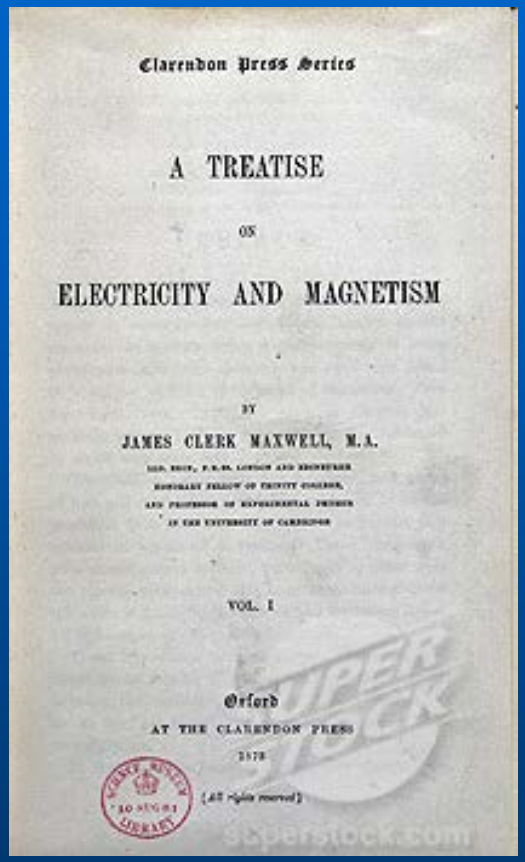
Clarendon Press Series

A TREATISE

ON

ELECTRICITY AND MAGNETISM

BY

JAMES CLERK MAXWELL, M.A.

VOL. I

Oxford

AT THE CLARENDON PRESS

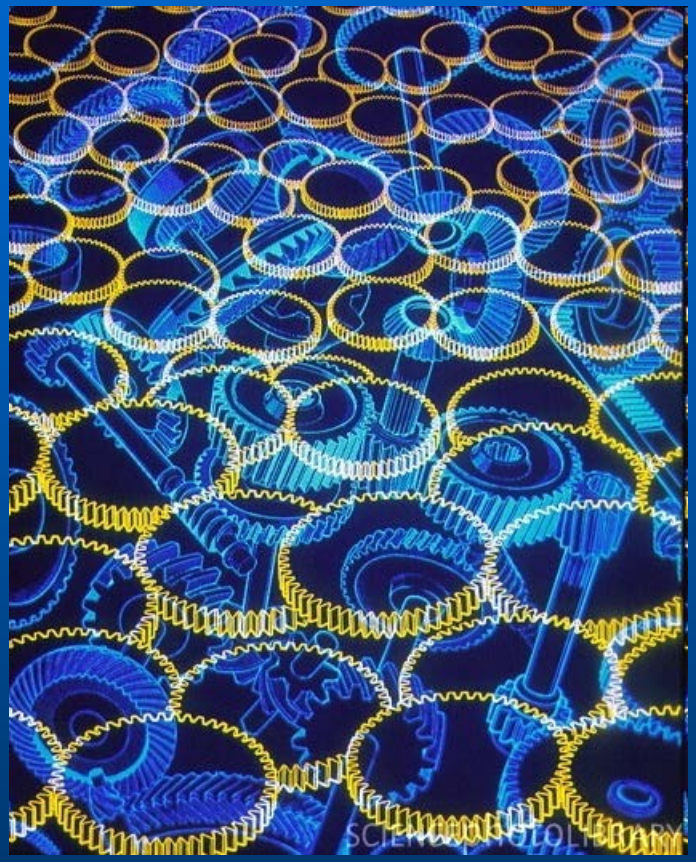

Electromagnetic fields as deformations in ether; gears and wheels

Review: Vozmediano, MIK & Guinea, Phys. Rep. 496, 109 (2010)

Zero-field QHE by strain engineering

F. Guinea, MIK & A. Geim, Nature Phys. 6, 30 (2010)

Can we create uniform (or almost uniform) pseudomagnetic field?

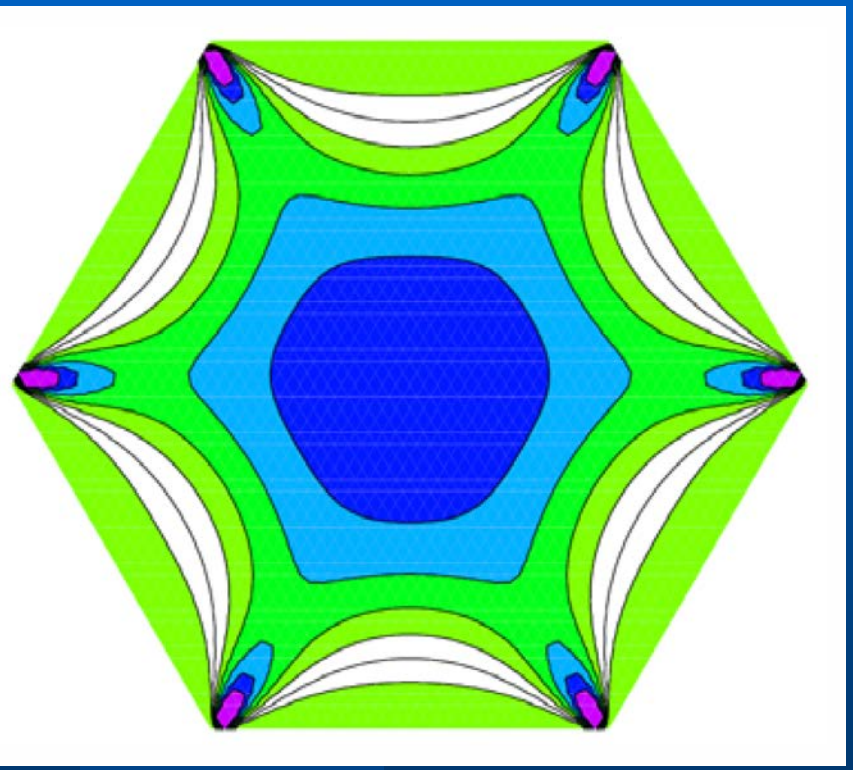

If you keep trigonal symmetry, quasi-uniform pseudomagnetic field can be easily created

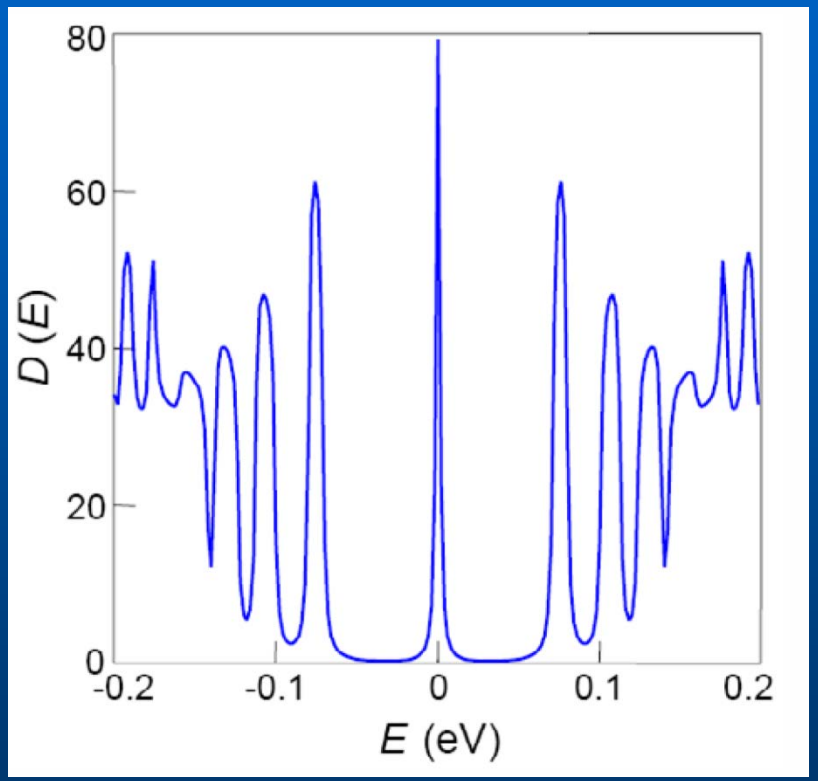

Normal stress applied to three edges size 1.4 μm, DOS in the center (0.5 μm)

Experimental confirmation

Strain-Induced Pseudo–Magnetic Fields Greater Than 300 Tesla in Graphene Nanobubbles

N. Levy,[1,2]*† S. A. Burke,[1]*‡ K. L. Meaker,[1] M. Panlasigui,[1] A. Zettl,[1,2] F. Guinea,[3] A. H. Castro Neto,[4] M. F. Crommie[1,2]§

30 JULY 2010 VOL 329 SCIENCE

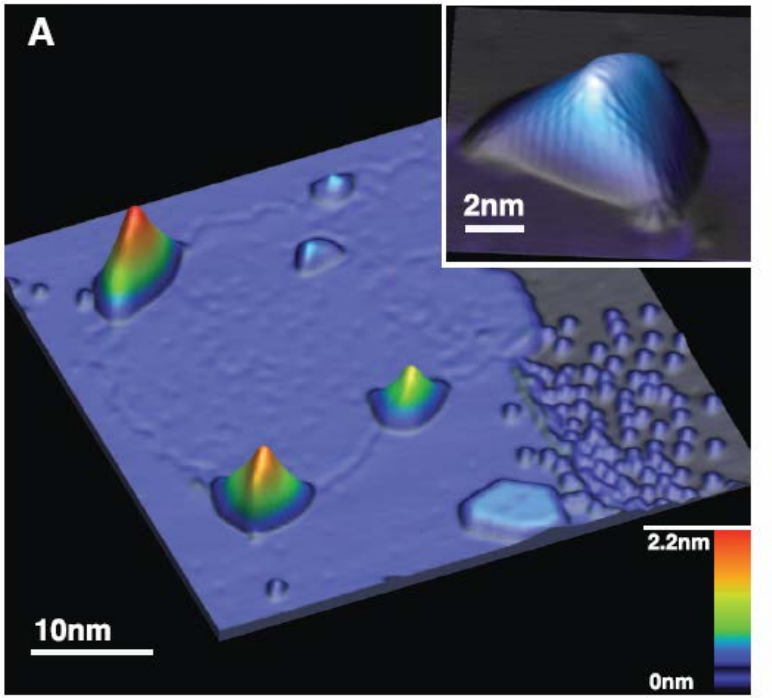

Graphene on Pt(111)

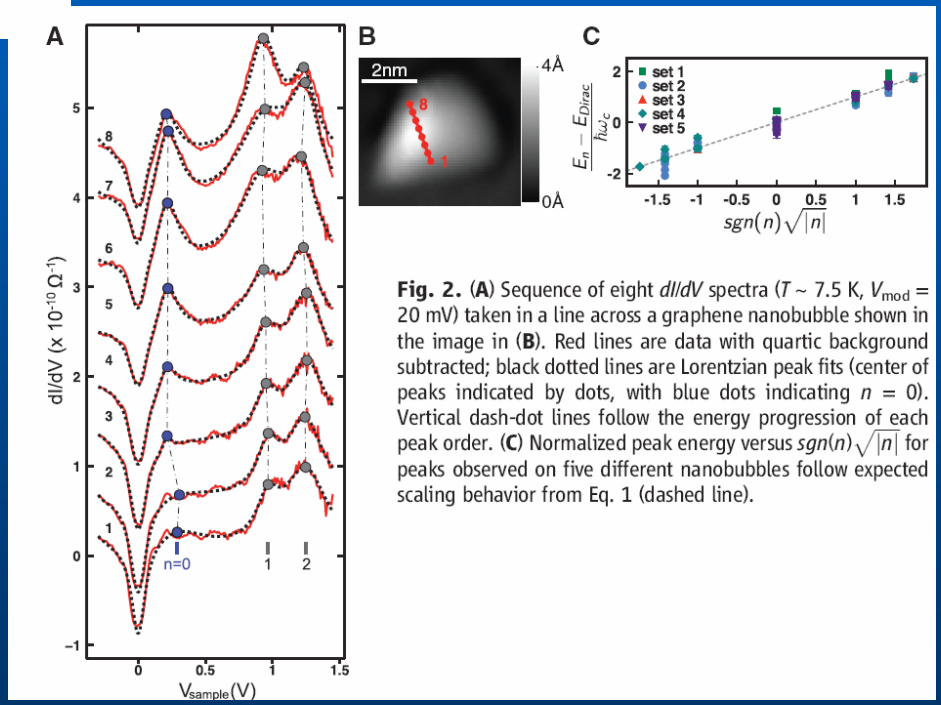

Fig. 2. (**A**) Sequence of eight *dI*/*dV* spectra (T ~ 7.5 K, V_{mod} = 20 mV) taken in a line across a graphene nanobubble shown in the image in (**B**). Red lines are data with quartic background subtracted; black dotted lines are Lorentzian peak fits (center of peaks indicated by dots, with blue dots indicating n = 0). Vertical dash-dot lines follow the energy progression of each peak order. (**C**) Normalized peak energy versus $sgn(n)\sqrt{|n|}$ for peaks observed on five different nanobubbles follow expected scaling behavior from Eq. 1 (dashed line).

STM observation of pseudo-Landau levels

Combination of strain and electric field: Haldane insulator state

T. Low, F. Guinea & MIK, PRB 83, 195436 (2011)

Without inversion center combination of vector and scalar potential leads to gap opening

$$\Delta = -\mathrm{Tr}\left\{\sigma_z \frac{2}{v_F}\int d^2\vec{\mathrm{k}} \frac{\mathrm{Im}\left(V_{-\vec{\mathrm{k}}}\right)\left[(\vec{\mathrm{k}}\vec{\sigma}),(\vec{\mathrm{A}}_{\vec{\mathrm{k}}}\vec{\sigma})\right]}{|\vec{\mathrm{k}}|^2}\right\}$$

$$\propto \int d^2\vec{\mathrm{k}} \frac{\mathrm{Im}(V_{-\vec{\mathrm{k}}})\left(k_x A^y_{\vec{\mathrm{k}}} - k_y A^x_{\vec{\mathrm{k}}}\right)}{|\vec{\mathrm{k}}|^2} \qquad (1)$$

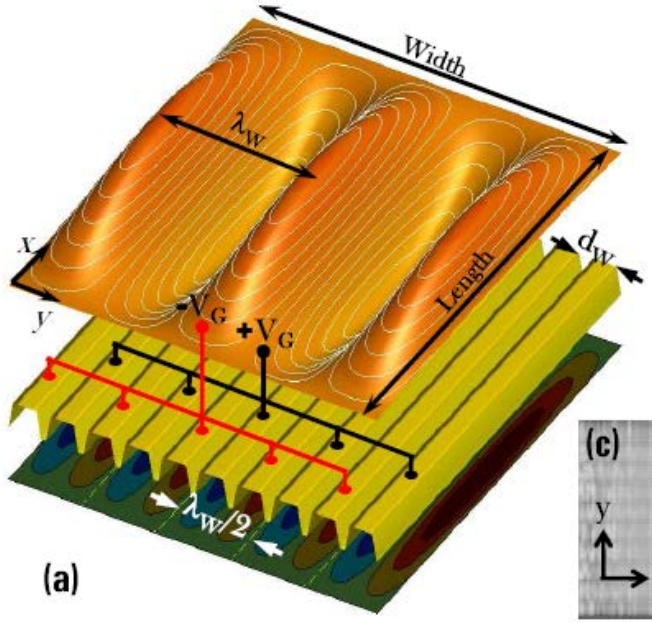

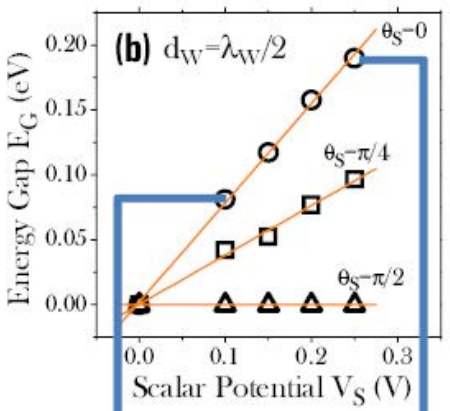

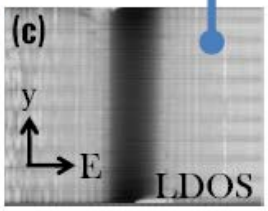

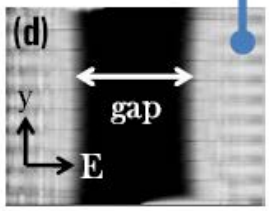

Wrinkles plus modulated scalar potential at different angles to the wrinkilng direction

Quantum pumping

T. Low, Y. Jiang, MIK & F. Guinea Nano Lett. 12, 850 (2012)

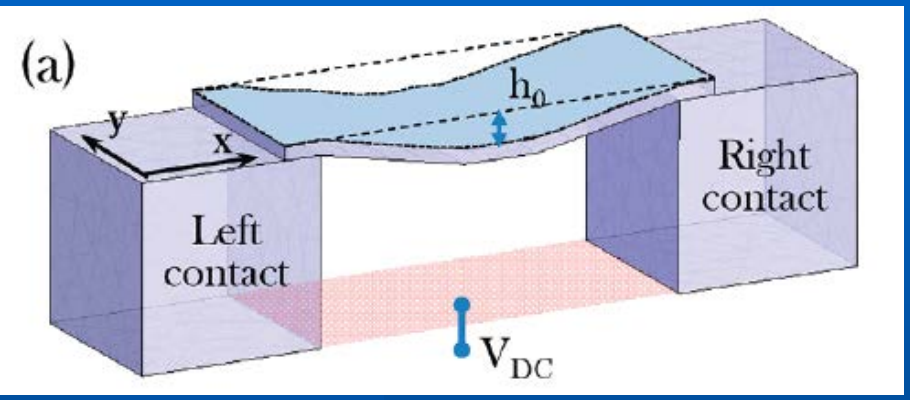

Nanoelectromechanical resonator, periodic change of electric fields and pseudomagnetic fields (deformations) – a very efficient quantum pumping

Periodic electrostatic doping *plus* vertical deformation $a(t)$ created pseudomagnetic vector potential

$$V(t) = V_{dc} + V_{ac}\cos(\omega t)$$

$$\varepsilon_d = \hbar v_f (\pi C_T V_{dc}/e)^{1/2}$$

$$\delta\varepsilon_d = V_{ac}/V_{dc}$$

$$u_{xx} = 8h_0^2/3L^2$$

$$\delta u_{xx} = a/h_0$$

$$\mathcal{E}_{dg}(t) = \varepsilon_d\{1 + \delta\varepsilon_d \sin(\omega t)\}^{1/2}$$

$$\mathcal{U}_{xx}(t) = u_{xx}\{1 + \delta u_{xx} \sin(\omega t + \phi)\}^2 - \frac{\Delta L}{L}$$

Quantum pumping II

Scattering problem

$$\psi_j(x) = \begin{cases} \begin{pmatrix} 1 \\ \eta_l \end{pmatrix} e^{ik_{xl}x} + \mathcal{R}_{\upsilon} \begin{pmatrix} 1 \\ -\eta_l^{\dagger} \end{pmatrix} e^{-ik_{xl}x} \\ \alpha_l \begin{pmatrix} 1 \\ \eta_g \end{pmatrix} e^{ik_{xg}x} + \alpha_g \begin{pmatrix} 1 \\ -\eta_g^{\dagger} \end{pmatrix} e^{-ik_{xg}x} \\ \mathcal{T}_{\upsilon} \sqrt{\dfrac{k_{xl}k_{fr}}{k_{xr}k_{fl}}} \begin{pmatrix} 1 \\ \eta_r \end{pmatrix} e^{ik_{xr}x} \end{cases}$$

Pumping current

$$\mathcal{I}_{\upsilon} = i\frac{e\omega}{4\pi^2} \sum_{k_y} \int_0^{2\pi/\omega} dt \int_{-\infty}^{\infty} d\varepsilon \frac{\partial f_0(\varepsilon)}{\partial \varepsilon} \Omega_{\upsilon}(k_y, t)$$

$$\Omega_{\upsilon} = (\partial \mathcal{T}_{\upsilon}/\partial t)\mathcal{T}_{\upsilon}^{\dagger} + (\partial \mathcal{R}_{\upsilon})/\partial t)\mathcal{R}_{\upsilon}^{\dagger}$$

Asymmetric leads (different doping)

Results

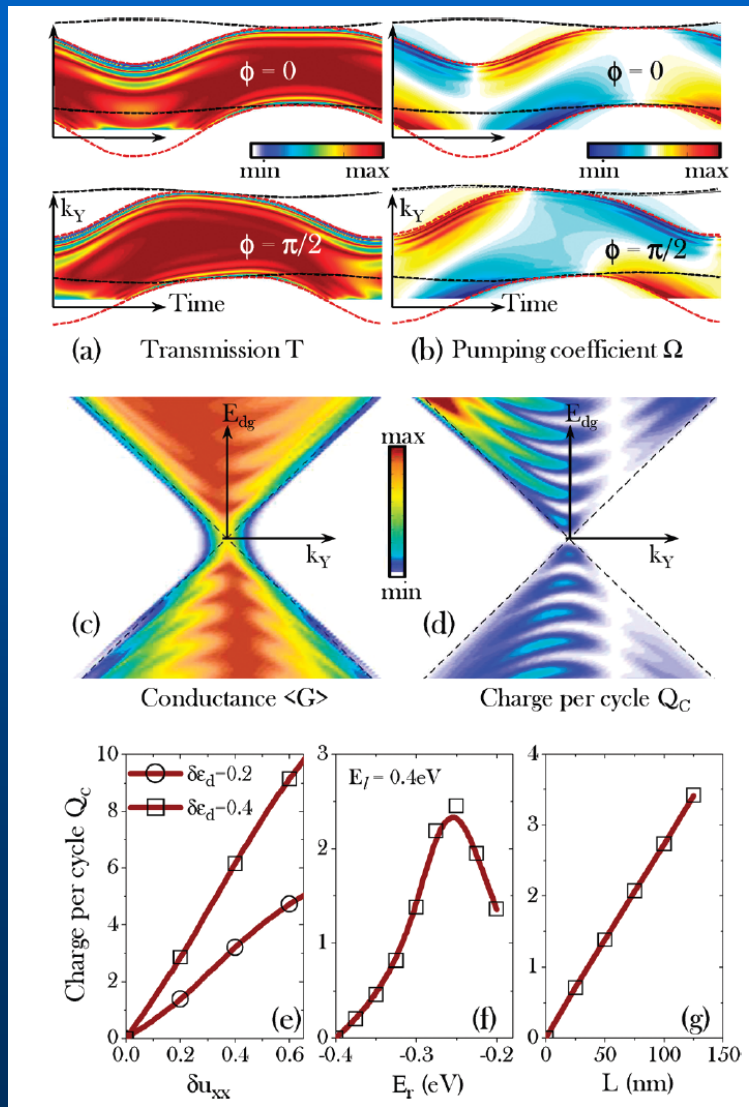

Collaborations

Sasha Lichtenstein and his group (Hamburg)
Olle Eriksson and his group (Uppsala)
Andre Geim, Kostya Novoselov and theirs group (Manchester)
Tim Wehling and his group (Bremen)

Sasha Shick (Prague), Alyosha Rubtsov (Moscow), Paco Guinea (Madrid), Leonya Levitov (MIT) and many others

And our group in Nijmegen